Presentazione e traduzione delle parti più significative della relazione geologica a firma del Prof. Gianluca Vignaroli et al. dal Titolo: "*Structural compartmentalisation of a geothermal system, the Torre Alfina field (central Italy)*" pubblicata sulla rivista scientifica specializzata "Tectonophysics" numero 608 pagg. 482-498.

Il lavoro (pubblicato nel 2013) ha come obiettivo principale lo studio della possibilità di alimentazione del campo geotermico di Torre Alfine da parte dell'affioramento di rocce carbonatiche del Monte Cetona (a Nord dell'area interessata). Il lavoro dimostra, in maniera inequivocabile la struttura a "compartimenti stagni" del serbatoio di rocce carbonatiche (attualmente interessato dai progetti geotermici) e come i sistemi di faglie parallele e di faglie normali del serbatoio carbonatico agiscono da barriera impermeabile al movimento orizzontale dei fluidi, escludendo, quindi, non solo la ricarica dal Monte Cetona, ma anche la interscambiabilità dei fluidi tra un "compartimento di rocce carbonatiche" e l'altro. Sotto questo ultimo aspetto lo studio appare valido per l'intero distretto vulcanico vulsino, caratterizzato dalla stessa struttura tettonica a "compartimenti stagni" del serbatoio di rocce carbonatiche.

Già nel sommario si dichiara (pag 482):

"post-orogenic deformation structures controlling the compartmentalisation of the Torre Alfina geothermal field. Strike-slip and subordinate normal fault systems (with associated network fractures) cut and dislocate the internal architecture of the reservoir and prevent its hydraulic connection ……..
The results have been used for illustrating a new geological conceptual model for the Torre Alfina area where the geothermal system is composed of different compartments. Tectonic structures define the main boundaries between compartments, helping the understanding of why productive and non-productive wells were found in apparently similar structural settings within the Torre Alfina field."

Traduzione: "le strutture di deformazione post-orogenetica dividono il campo geotermico di Torre Alfine in compartimenti . I sistemi di faglie parallele e subordinate faglie normali (con le annesse reti di fratture) tagliano e slegano la struttura interna del serbatoio ed impediscono la sua continuità idraulica…..
I risultati dimostrano un nuovo modello geologico concettuale per l'area di Torre Alfina dove il sistema geotermico è composto di distinti compartimenti. Le strutture tettoniche delimitano i confini principali tra i compartimenti, facendo capire perché,all'interno del campo di Torre Alfina, si trovano pozzi produttivi accanto ad altri sterili in una struttura apparentemente simile"

E nell'introduzione (# 1) (pag 482):

"It has been demonstrated that the interplay between deformation, fracturing and sealing may generate a complex fluid-rock pattern in both active and fossil tectonic settings (Cox et al., 2001; Oliver, 1996; Rossetti et al., 2011; Rowland and Sibson, 2004; Sheldon and Ord, 2005; Sibson, 2000), including near vertical channelized fluid flows along unsealed discontinuities (e.g. Cas et al., 2011; Sibson, 2000) and limited horizontal fluid migrations within fault-barriers rock-bounded (e.g. Faulkner and Rutter, 2001)".

Traduzione: "È stato dimostrato che la combinazione di deformazione, fatturazione e saldatura può generare un complesso rapporto fluido-roccia sia in una tettonica attiva sia in una fossile (Cox et al., 2001; Oliver, 1996; Rossetti et al., 2011; Rowland and Sibson, 2004; Sheldon and Ord, 2005; Sibson, 2000), compresa la canalizzazione quasi verticale dei fluidi lungo discontinuità non saldate (e.g. Cas et al., 2011; Sibson, 2000) ed un limitato scorrimento orizzontale dei fluidi tra blocchi di roccia delimitati da faglie-barriera (e.g. Faulkner and Rutter,2001)"

Dopo un accurato studio sui Lineamenti Geologici della Zona (# 2), Il Rilevamento di Campagna e lo Studio delle Strutture di Fratturazione(# 3), della Geocronologia(# 4), e dell'Analisi degli Andamenti dei Lineamenti Strutturali(# 5), nella Discussione (# 6) si precisa (pag 492):
"It has been also demonstrated that deformation zones may also act as hydraulic barriers to fluid flow (e.g. Faulkner and Rutter, 2001), as effect of rock comminution during fault slip or secondary mineralization".

<u>Traduzione</u>: "È anche stato dimostrato che le zone di deformazione possono anche agire da barriera allo scorrere dei fluidi (e.g. Faulkner and Rutter, 2001),come effetto dell'alterazione della roccia nello scorrere della faglia o della sua mineralizzazione secondaria"

Ed ancora (#6-3)(pag. 495):

"from numerical models for fluid convection (e.g. McLellan et al., 2010; Oliver et al., 2006), we assume that tectonic discontinuities
in Torre Alfina area may have a double role: (i) as main paths of fluids in vertical sense, connecting different structural levels of the geothermal rock system and favouring the advection flow; and (ii) as main barriers for the horizontal motion of fluids, disconnecting the circulation at the same structural level. These features argue for a largely heterogeneous secondary permeability in a compartmentalised reservoir. The occurrence of randomly unproductive or very productive deep bore-holes within the same reservoir should be explained in these terms.

<u>Traduzione</u>: da modelli matematici della convezione dei fluidi (e.g. McLellan et al., 2010; Oliver et al., 2006), presumiamo che le discontinuità tettoniche nell'area di Torre Alfina possano avere una duplice funzione: (1) di canale preferenziale per l'ascesa dei fluidi verticalmente, mettendo in comunicazione livelli strutturali differenti di rocce del sistema geotermale e facilitando il flusso di adduzione; (2) di principale barriera al flusso orizzontale dei fluidi, interrompendo la circolazione in uno stesso livello strutturale. Queste caratteristiche sono a favore di una permeabilità secondaria molto eterogenea in un serbatoio fatto a compartimenti. La presenza casuale, nello stesso serbatoio, di perforazioni profonde sterili o molto produttive, andrebbe spiegata per queste ragioni.

Infine nelle Conclusioni (# 7) si dichiara (pag 496):

"Torre Alfina represents a key area for studying the effect of the tectonic deformation and its role on the geothermal system. Distribution, persistence, and geometry of the tectonic structures affect the fluid flow within the Torre Alfina geothermal system that can be imaged as composed of different compartments with inhomogeneous fluid network. Tectonic structures define the main boundaries between compartments, helping the understanding of why productive and non-productive wells were found in apparently similar structural settings within the Torre Alfina field".

<u>Traduzione</u>: Torre Alfina rappresenta un'area fondamentale per studiare l'effetto della deformazione tettonica ed il suo ruolo nel sistema geotermale. Distribuzione, insistenza e geometria delle strutture tettoniche determina lo scorrere dei fluidi all'interno del sistema geotermico di Torre Alfina che può essere immaginato come composto di differenti compartimenti interessati da una rete disomogenea di fluidi. Le strutture tettoniche delimitano i principali limiti tra compartimenti, aiutando a capire perché nel campo geotermico di Torre Alfina si trovano, in situazioni strutturali apparentemente simili pozzi produttivi e pozzi sterili.

CONCLUSIONI

L'area in oggetto è ad alto rischio sismico con centri storici particolarmente sismo vulnerabili (si ricordano i terremoti di Tuscania e di Castel Giorgio). Le rocce carbonatiche interessate dallo sfruttamento geotermico fanno parte geologicamente e tettonicamente della stessa struttura appenninica dove si è verificato il 24/8/17 e seguenti il catastrofico sisma di Amatrice-Monti Sibillini, da cui è separata dalla depressione tettonica dove scorre il fiume Tevere. In linea d'aria dista meno di 100 km. È legittimo presumere che travasando in modo permanente grandi quantità di fluidi da un compartimento ad un altro senza che fra essi vi sia continuità idraulica, si crei depressione in uno e pressione nell'altro. Si favoriscono in tal modo i movimenti delle faglie innescando terremoti. Il travaso permanente facilita inoltre la risalita di fluidi geotermici (cancerogeni) verso l'acquifero superficiale.

Dott. Geologo Mario Mancini

Allegato C1.1
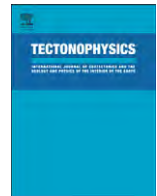
Structural compartmentalisation of a geothermal system, the Torre Alfina field (central Italy)

Gianluca Vignaroli *, Annamaria Pinton, Arnaldo A. De Benedetti, Guido Giordano, Federico Rossetti, Michele Soligo, Gabriele Berardi

Dipartimento di Scienze, Università Roma Tre, Viale Marconi, 446, 00146 Roma, Italy

ARTICLE INFO

ABSTRACT

Recent surging of renewed industrial interest in the exploration of low and medium enthalpy geothermal fields makes the accurate assessment of the geothermal potential essential to minimise uncertainties during both exploration and exploitation. The Torre Alfina field is a case of abandoned, but promising, geothermal field of central Italy where the roles of the internal structural setting and of the recharge areas on the hydrothermal circulation are largely unconstrained. In this paper, field structural data integrated with geomorphic lineament analysis document the occurrence of post-orogenic deformation structures controlling the compartmentalisation of the Torre Alfina geothermal field. Strike-slip and subordinate normal fault systems (with associated network fractures) cut and dislocate the internal architecture of the reservoir and prevent its hydraulic connection with Mount Cetona, considered to be the recharge area and where hydrothermal manifestation, including travertine deposition, occurs. ^{230}Th/^{234}U radiometric dating of superposed travertine units gives 200, 120 and 90 ka respectively, inferred to correspond to the age of the fossil hydrothermal circulation during tectonic activity. The results have been used for illustrating a new geological conceptual model for the Torre Alfina area where the geothermal system is composed of different compartments. Tectonic structures define the main boundaries between compartments, helping the understanding of why productive and non-productive wells were found in apparently similar structural settings within the Torre Alfina field.

© 2013 Elsevier B.V. All rights reserved.

1. Introduction

Geothermal energy resources are expected to play an increasing role on the future power demand, addressing large incentives from policymakers and capturing the attention of industries. A renewed world-wide interest for geothermal energy is also presently stimulated by technological advances in exploration and exploitation of medium-enthalpy systems.

Geophysical methods (e.g. Árnason et al., 2010; Bibby et al., 1995; Garg et al., 2007; Jousset et al., 2011; Newman et al., 2008), together with expensive explorative drillings, are commonly used for assessing the configuration of the main geothermal components (reservoir units, seal rocks, recharge area), as well as the characteristics and the hydrodynamic network of the endogenous fluids. An accurate interpretation of geophysical data depends on the reliability of the geological conceptual model of the investigated geothermal system. In particular, reconstruction of the geothermal setting is invariably connected with the geological history of the site, and evaluation of the main geological features in the area is a primary goal before planning the exploration. The incorrect definition of the geological model can lead to main failures

both in the exploration stage and during the exploitation of the geothermal field.

Fluid circulation depends on the permeability contrast in a reservoir, which favours the localisation of subsurface thermal anomalies (e.g. Guillou-Frottier et al., 2013; McLellan et al., 2010). In addition, geothermal reservoirs are usually described in areas with active tectonism, with fault systems and fracture networks perturbing the circulation of endogenous fluids and localising the hydrothermal manifestations at the surface (e.g. Barberi et al., 1984; Giordano et al., 2012; Kaven et al., 2011; Traineau et al., 1997; Wood, 1994). It has been demonstrated that the interplay between deformation, fracturing and sealing may generate a complex fluid-rock pattern in both active and fossil tectonic settings (Cox et al., 2001; Oliver, 1996; Rossetti et al., 2011; Rowland and Sibson, 2004; Sheldon and Ord, 2005; Sibson, 2000), including near vertical channelized fluid flows along unsealed discontinuities (e.g. Cas et al., 2011; Sibson, 2000) and limited horizontal fluid migrations within fault-barriers rock-bounded (e.g. Faulkner and Rutter, 2001).

Central Italy is characterised by a great number of geothermal fields that have been successfully exploited since the last century (e.g. Barberi et al., 1994). Larderello system is the best known example, but the presence of fossil and active hydrothermal manifestations distributed all along the Tyrrhenian margin has renewed the economic interest by private companies. Consequently, a large number of new research

* Corresponding author. Tel.: +39 0653778043; fax: +39 0657338201.
E-mail address: gianluca.vignaroli@uniroma3.it (G. Vignaroli).
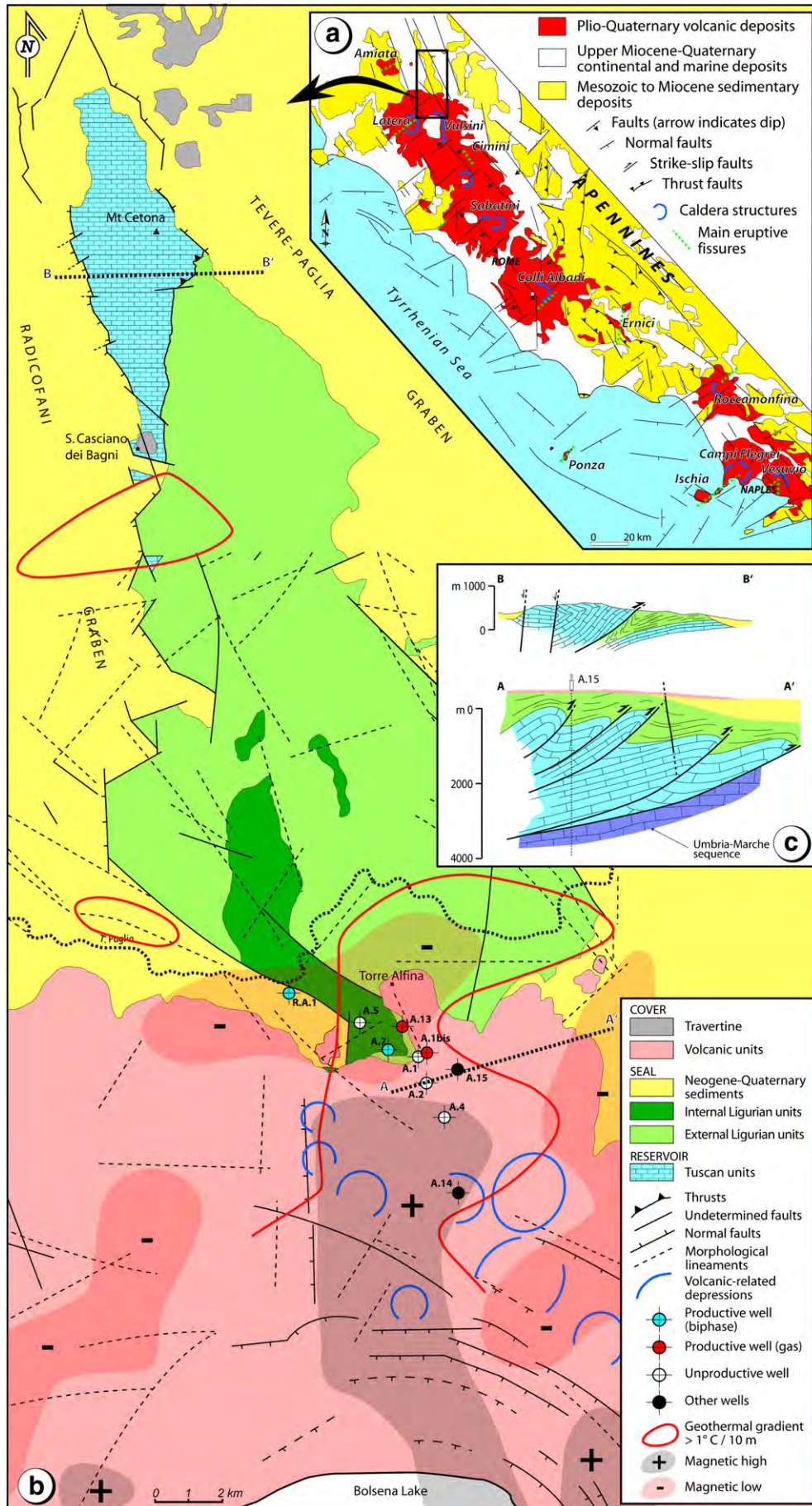
permits have been requested in the last two years for exploitation of different geothermal systems. Among these, the Torre Alfina area is an example of an early explored and subsequently abandoned geothermal field. This field was involved in geological–geophysical studies with geothermal purposes since the 1970s (e.g. Barberi et al., 1994; Buonasorte et al., 1988, 1991; Chiarabba et al., 1995; Chiodini et al., 1995; Costantini et al., 1984; Doveri et al., 2010). Fifteen deep boreholes were drilled with a series of failures as they apparently randomly resulted unproductive or very productive within the same reservoir. These data were used to assess the geological architecture of the deep reservoir of the Torre Alfina area, attributed to a N–S structural high inherited from the fold–thrust-belt construction of the Apennine belt (Buonasorte et al., 1987b).

The Torre Alfina field (Fig. 1) constitutes an ideal case history for studying the structural/tectonic control on the geothermal system architecture, inasmuch as: (i) the geothermal anomaly is localised in correspondence of a buried reservoir, (ii) the reservoir crops out north of the geothermal field, at the San Casciano dei Bagni village where evidence of fossil and active hydrothermalism occurs with sulphur springs and travertine deposition, and (iii) the San Casciano dei Bagni reservoir is located at the southern termination of the Mount Cetona ridge, classically considered to be the recharge area of the geothermal system (Buonasorte et al., 1988). In this work, we approach the geothermal potential and hydrothermal setting of the Torre Alfina area aimed at clarifying some still unanswered questions about its internal structural setting and its hydrothermal connection with neighbouring areas. We based our study through the reinterpretation of available geological data and we produced an original multidisciplinary dataset based on a field structural survey. Structural analyses were carried out in order to define the main tectonic features and associated fracture pattern in the areal extent of the geothermal field and in the surrounding Mount Cetona region. Such data were integrated with lineament detection on digital elevation models (DEMs) allowing generalisation of the structural trends at regional scale. Furthermore, we performed ^{230}Th/^{234}U radiometric dating of travertine concretions filling fossil hydrothermal circuits in the Mount Cetona area in order to provide insights on the space–time migration and distribution of hydrothermal circulation in the study area. Integration of the results allows us to propose a new geological model for the geothermal field that images the Torre Alfina area as a geothermal system composed of different structural compartments, where tectonic structures play a key role in producing renewed permeability distribution (that we refer as secondary permeability) and hydrothermal circulation/properties of the reservoir and its recharge pathways. Our data demonstrate the necessity to detail the structural setting of a geothermal area for assessing the configuration of the main geothermal components, as well as the hydrodynamic network of the endogenous fluids.

2. Geological setting

The present-day occurrence of medium- and high-enthalpy geothermal fields in central Italy is localised along the Tyrrhenian margin of the Apennines where the Pliocene–Quaternary magmatism affected the thinned orogenic crustal section (e.g. Argnani and Savelli, 1999; Faccenna et al., 1997; Jolivet et al., 1998; Kastens et al., 1988; Malinverno and Ryan, 1986; Peccerillo, 2003; Rosenbaum et al., 2008; Savelli, 2001; Serri, 1997; Fig. 1a). Post-orogenic extensional and strike-slip structures dissect the fold-and-thrust architecture of the Apennines (e.g. Barchi et al., 1998; Carmignani et al., 1994; Jolivet et al., 1998). A close relationship between the volcanic activity

(including hydrothermal manifestations) and the arrangement of post-orogenic structures has been clearly documented (e.g. Acocella and Funiciello, 2006; Acocella and Rossetti, 2002; Annunziatellis et al., 2008; Bellani et al., 2004; Brogi and Fabbrini, 2009; Buonasorte et al., 1987a; Chiodini et al., 1995; Faccenna et al., 1994b; Funiciello and Giordano, 2010; Funiciello et al., 1976; Giordano et al., 2006; Jolivet et al., 1998; Liotta, 1994; Liotta et al., 2010; Rossetti et al., 2008). Fig. 1a illustrates how calderas and main eruptive fissures are aligned along the main post-orogenic lineaments.

The Torre Alfina area is located to the north of the Vulsini calderas (Buonasorte et al., 1988), and it is comprised between the Meso-Cenozoic ridge of the Mount Cetona (Passerini, 1964), to the north, and the Bolsena caldera structure, to the south (Nappi et al., 1995) (Fig. 1b).

In the Torre Alfina geothermal system it is commonly accepted that:

a) the reservoir units are composed, from bottom to top, of evaporites, limestones, marls and radiolarites (Upper Triassic–Upper Cretaceous Tuscan series; Costantini et al., 1984). The reservoir units occur below the geothermal field in the Torre Alfina area where they are buried by the seal units, but also crop out at the San Casciano dei Bagni village;

b) the seal units consist of allochthonous flysch-type sequence composed of arenaceous turbidites intercalated with layers of shales, marls, and limestones, overlaid by an ophiolitic sequence (siliceous shales and sandstones including blocks of gabbros, serpentinites) (Lower Cretaceous to Upper Eocene Ligurian units s.l.; Carmignani and Lazzarotto, 2004);

c) the heat source is provided by the Pliocene–Quaternary volcanism of the Vulsini area (Barberi et al., 1994). Volcanics unconformably overlie the allochthonous flysches and the Miocene–Pliocene marine sediments that filled the extensional basins (Radicofani and Paglia–Tevere grabens);

d) the recharge area is commonly referred to the Mount Cetona (Buonasorte et al., 1988), a N–S tectonic ridge composed of Mesozoic–Cenozoic sequence belonging to the Tuscan series.

The integration of geophysical (Buonasorte et al., 1988, 1991) and seismic (Chiarabba et al., 1995) data identified a buried structural high in the Torre Alfina area, marked by the convergence of positive geothermal (geothermal gradient >1 °C/10 m) and magnetic anomalies (Fig. 1b). Most of the deep bore-holes were drilled on top of this structure. Interpretation of the "Alfina 15" well indicates the tectonic stacking of Tuscan and Ligurian units controlled by W-dipping thrust systems (Buonasorte et al., 1991) (cross-section A–A' in Fig. 1c).

The Tuscan units that make up the Mount Cetona structure are arranged to form a large overturned-to-recumbent anticline, trending NNW–SSE. Following Passerini (1964), the Cetona Tuscan sequence westward overthrusts the allochthonous Ligurian units (see geological cross-section B–B' in Fig. 1c). On the other hand, Piscopo et al. (2009) recognised seven deformation phases responsible for the present-day setting of the Mount Cetona and interpreted the Cetona structure as a horst bounded by N–S striking post-orogenic extensional faults. Spring waters sampled within the Cetona ridge and at the San Casciano dei Bagni indicate hydrochemical and isotopic composition heterogeneity (Piscopo et al., 2009) suggesting the presence of a sectorial fluid circulation. The contrasting geological interpretations and the hydrogeochemical evidence question models of continuous hydraulic connection and make it disputed the role of the Mount Cetona as the recharge area of the Torre Alfina geothermal system.

Fig. 1. (a) Structural map of the Tyrrhenian margin of central Italy showing the main tectono–stratigraphic domains and the regional fault arrays (Acocella and Funiciello, 2006, redrawn and modified); (b) geological map of the Torre Alfina geothermal system and adjoining areas, integrated with geophysical data (Buonasorte et al., 1988; Carmignani and Lazzarotto, 2004; Costantini et al., 1984; Passerini, 1964; redrawn and modified). The locus of exploitation wells is also shown; (c) cross-section A–A' shows the Meso-Cenozoic ridge of the Mt Cetona overthrusting the allochthonous flysch along N–S thrust system (Passerini, 1964, redrawn); and cross-section B–B' illustrates the deep structure in the Torre Alfina area (Buonasorte et al., 1991, redrawn).
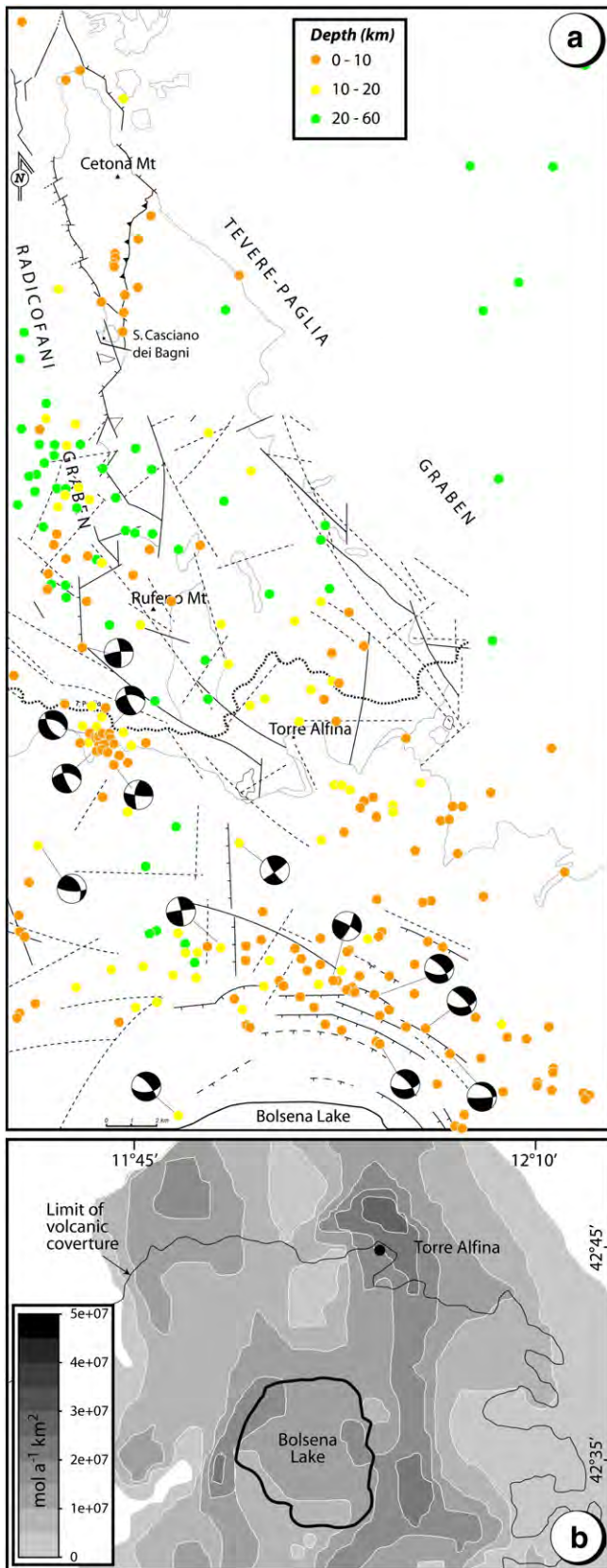
Fig. 2. (a) Locus of epicentres for earthquakes that occurred in the study area in 2005–2012 period (downloaded from ISIDE, Italian Seismological Instrumental and Parametric Data-Base, INGV; http://iside.rm.ingv.it) with focal mechanisms after Buonasorte et al. (1987a); (b) map of the CO$_2$ flux deduced from groundwater analyses from the area between Torre Alfina and Bolsena Lake (Gambardella et al., 2004, redrawn and modified).

The area between the Bolsena Lake and the Mount Cetona is characterised by both deep and shallow seismicity (Fig. 2a). Large amounts of hypocenters are concentrated within 15–25 km and <10 km crustal depths. In the upper crust levels, hypocenters are distributed in the 3–11 km depth. The record of recent seismicity in the northern Vulsini Mountains (2005–2012 period, http://iside.rm.ingv.it; Fig. 2a) resembles the seismicity recorded in the 1977–1986 period in terms of magnitude (all events are less than 3.5) and of epicentre location. Low-magnitude seismicity is diffuse in the area, although a tendency to be located externally to the carbonate structural high below the Torre Alfina can be observed. In particular, shallow hypocenters (less than 10 km) are associated with fault-step calderic depression of the Bolsena Lake and the fault zone bounding the eastern flank of the Radicofani Basin (between the Mount Cetona and the Acquapendente village). Buonasorte et al. (1987a) put in evidence the consistency of this seismicity with three main tectonic directions: NE–SW, NW–SE, and E–W. Although geometry, orientation, and kinematics of tectonic structures occurring in the Torre Alfina geothermal system have not yet been studied in detail, available focal mechanisms show strike-/oblique-slip and/or normal solutions along E–W and NNE–SSW oriented faults (Buonasorte et al., 1987a).

CO$_2$ dissolved in the shallow groundwaters of the northern Vulsini volcanoes shows anomalous values aligned along a N–S direction, from the Bolsena Lake to the Torre Alfina area (Gambardella et al., 2004; Fig. 2b). This suggests the occurrence of a hydraulic connection within a, presumably, continuous aquifer distributed south of the Torre Alfina area.

3. Structural field study

The field surveys were performed in the geothermal area (the Torre Alfina area) and in the area where the exposed reservoir (at the San Casciano dei Bagni) meets the Mount Cetona ridge. The analysis was applied to tectonic discontinuities (faults and fracture systems) that show evidence of post-orogenic activity. The structures were studied in terms of geometric (spacing, aperture, and persistence) and kinematic features. The results of our field investigations are synthesised in geological-structural maps (Figs. 3 and 9a) and are presented as stereographic projections (Figs. 4 and 9b).

In the Torre Alfina area we focused on structures affecting Quaternary volcanic deposits (tephritic lavas and pyroclastites). These structures were compared with the deformation fabrics of the allochthonous flysch units, in order to discriminate the recent fault/fracture pattern that affects the seal units. This allows us to individuate the main pathways that affect the circulation of the endogenous fluids from the buried reservoir to the surface.

The geometric–structural relationships of the reservoir units were investigated at the Mount Cetona and the San Casciano dei Bagni, with the aim to have insights on the hydraulic connection between the geothermal field and the attributed recharge area. We performed detailed structural investigations in the area corresponding to the structural link between the recumbent anticline structure at the Mount Cetona and the normal stratigraphic polarity at the San Casciano dei Bagni. Here, we analysed structures in the carbonate reservoir coexisting with travertine deposition.

3.1. The Torre Alfina area

More than 700 structural data relative to brittle deformation features have been collected in the Torre Alfina area. These data are faults showing strike-, oblique- and dip-slip kinematics, associated with fractures and mineralized veins.

In layered pyroclastites, NNE–SSW-striking shear zones are composed of spaced fractures evolving to pervasive fault systems (Fig. 5a, b; structural stop no. 14). Fractures are both tensile- and shear-fractures (mode-I and mode-III of Atkinson, 1987, respectively).
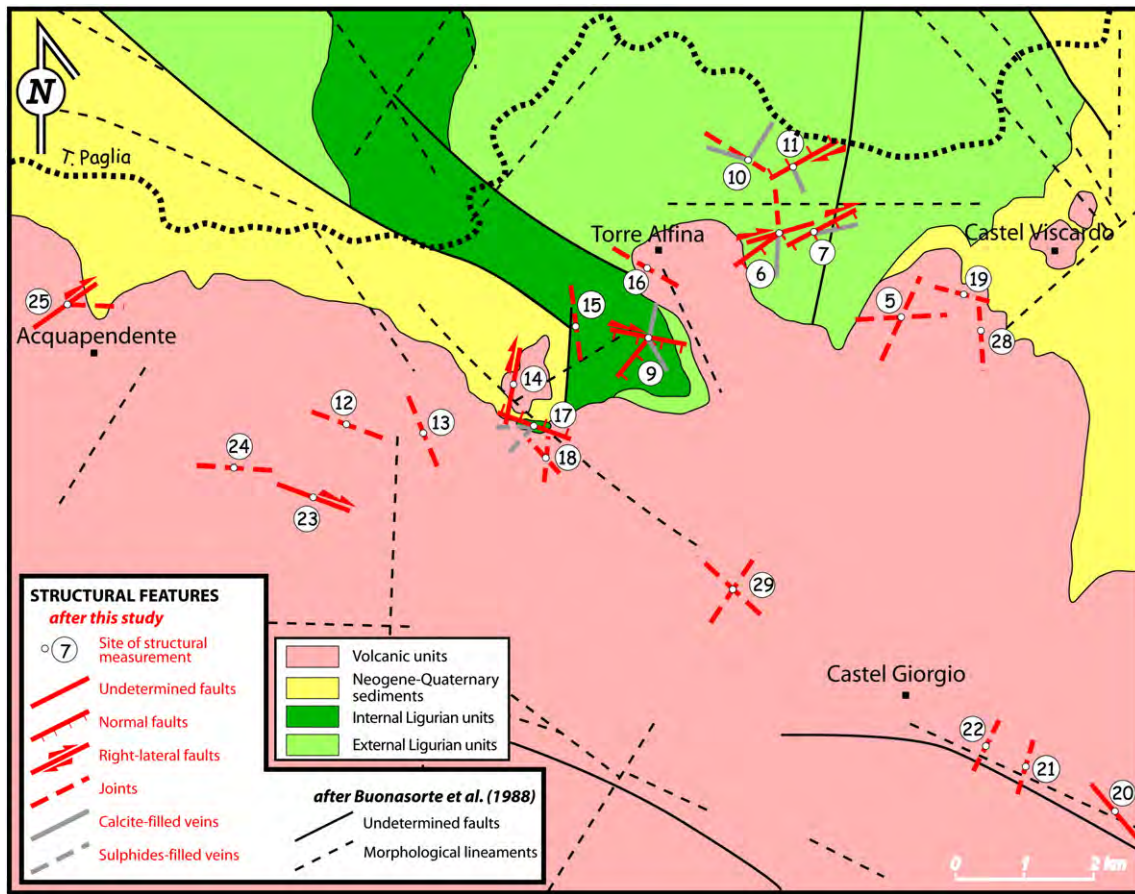
Fig. 3. Structural map of the Torre Alfina area with location of the structural stops. Spatial distribution of structural features after Buonasorte et al. (1988) is also reported.

Fractures are sub-vertical and show variable persistence from few decimetres to more than 5 m. Decimetre-sized fractures develop within competent cineritic layers and disappear at the boundaries with granular layers, seldom showing centimetric offset (Fig. 5c). Longer fractures dissect through all along the pyroclastic sequence (Fig. 5d), showing increase of aperture and offset moving upwards along the discontinuity plane. Fractures strike sub-parallel, but their spacing decrease moving to the fault zone. Fault planes strike NNE–SSW and they are sub-vertical or highly dipping to eastern quadrants. Slickenlines on fault planes (see insert in Fig. 5e) have a pitch less than 20° or more than 160°. The damaged thickness in fault zones can be up to 2 m and its architecture consists of main shear surfaces and subsidiary Riedel planes (Fig. 5e). The analysis of shear criteria (e.g. Petit, 1987) documents dextral strike-slip movement.

WNW–ESE shear zones in pyroclastites (Fig. 6a, b) appear less developed with respect to NNE–SSW shear zones. Fractures have a mainly tensional attitude and do not show appreciable offsets. Spacing between fractures is less regular and variable from few decimetres to 1 m. Fractures strike parallel to the main fault planes (Fig. 6c) that define metric damage zone. The internal architecture of the damage zone includes curvilinear shear surfaces making an angle of 15–20° with the main strike of the main fault plane and interpreted as Riedel shears. A dominant strike-slip motion (slickenlines pitch less than 20° or more than 160°) with dextral kinematics has been observed. Oxides are the principal mineral phases detected on fault surfaces in volcanic rocks.

Tensional fractures have been recognised in lavas (structural stop nos. 5, 18, 19, 20, 28, 29; Fig. 7a, b). Fractures of tectonic origin have been discriminated by discontinuities of uncertain origin (for example due to lava cooling) by considering their geometrical properties

(spacing, persistence, and aperture) and their angular relationships with fault systems. Fracture surfaces are mainly planar often showing irregular tip terminations; any appreciable mineralisation has been detected within the discontinuities. These show systematic increase of aperture (from few centimetres to half metre) shifting from low- (less than 1 m) to high-persistence (plurimetric). Statistical analysis of collected data allows grouping the fractures into NNE–SSW and WNW–ESE main directions, both of them with sub-vertical attitude (Fig. 7).

The most recurrent structures in flysch deposits (Ligurian units s.l.) outcropping close the Torre Alfina village consist of fault segments striking NE–SW (structural stop nos. 6, 7, 11) to E–W (structural stop nos. 9 and 17), frequently associated with tensional joints. Major faults show rough planar slip surfaces without occurrence of appreciable mineralisation. Faults evolve into shear zones (Fig. 8a–c) producing metric scale damage zones (i.e. the rock volume affected by fault-related fracturing; e.g. Caine et al., 1996). Slickenlines on fault planes (Fig. 8d, e) often show the superimposition of oblique slip motion (slickenline pitch less than 45° and over 135°) on dip-slip motion (slickenline pitch between 70° and 120°). The interpretation of the kinematic indicators at the meso-scale (striation, lunate fractures, Riedel planes; cfr. Petit, 1987) suggests a transtensional deformation regime. Curvilinear fault segments describe anastomosed geometry and sigmoid lithons compatible with a normal sense of shear (Fig. 8f). Mineralized joints are present at the footwall of the low angle normal faults (structural stop no. 17). Joints are high dipping to sub-vertical (Fig. 8g) and show composite mineralisation consisting of external sulphides rim and internal clay agglomerates (Fig. 8h). Evidence of fluid percolation in the shear zone is also typified by large patches of sulphides all along the fault planes. A complex structural network of
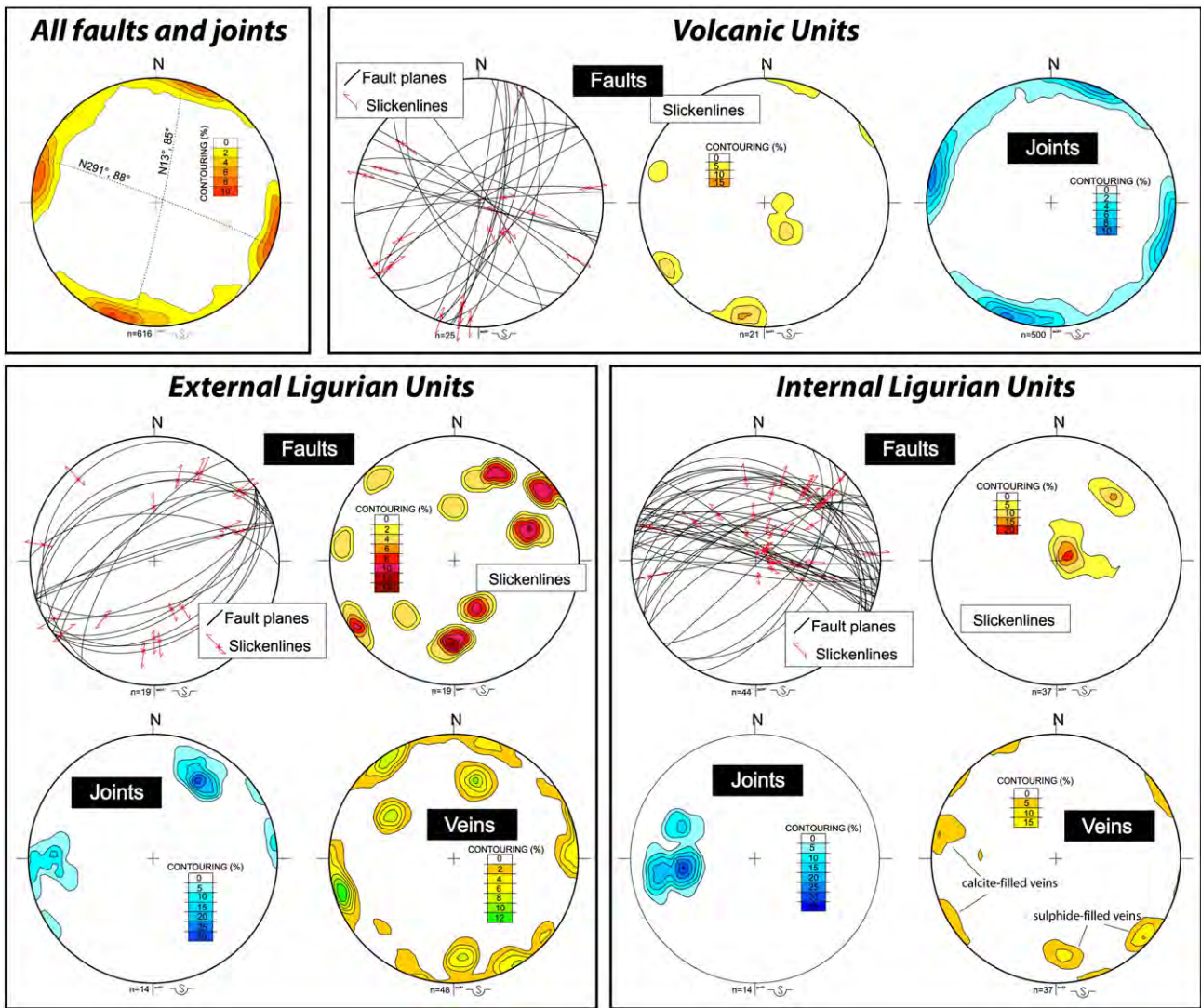
Fig. 4. Stereographic projections (Schmidt net, lower hemisphere) of the data collected in Ligurian (both internal and external) and volcanic units.

mutual intersecting fractures and veins has been also recognised in the fault damage zone. Here, calcite-filled veins systematically cut the syn-orogenic features (represented by pressure-solution seams) and show crystals growing perpendicular to the vein walls. These veins, which strike from NNE–SSW to E–W, have sharp and rectilinear shape, with centimetric thickness.

3.2. The Cetona–San Casciano dei Bagni area

Between the Cetona ridge and the San Casciano dei Bagni area, the Middle Jurassic to Upper Cretaceous Tuscan series forms a complex kilometre-sized structure. At the Cetona ridge, the recumbent flank of the anticline is disposed in monoclinal geometry and dips to the west (Fig. 9a). The Tuscan units are overthrusted on the arenaceous turbidites of the Ligurian flysch, in agreement with the early work of Passerini (1964). In the field, this contact corresponds to a 20–25° westward dipping thrust plane. The thrust plane is marked by both ductile deformed strata in close-to-isocline N–S folds and half metre thick cataclastic horizon. Close to the San Casciano dei Bagni, the same Tuscan series displays a normal stratigraphic polarity (Fig. 9) and dips to the east below the flysch sequence (Passerini, 1964; Piscopo et al., 2009).

In the area where the recumbent anticline structure passes to the normal stratigraphic polarity, the carbonates show domains of intense tectonic deformation (Fig. 10a) that obscure the pristine sedimentary fabric. Extensional fractures are organised in both systematic and non-systematic sets. In non-systematic sets (Fig. 10b), the fractures are mainly represented by veins filled by both spatic and globular calcite. Veins show a random spatial distribution, characterised by both low and high dip angles. Veins have thickness ranging from 1–2 cm to 10 cm. Multiple intersections between veins shape polygonal lithons with size ranging from few centimetres to half metre. Persistence of veins in non-systematic sets is low, with discontinuity trace lengths not higher than half metres. Discontinuities which terminate against other discontinuities are the most common features in this deformation field.

In systematic sets, two main directions can be obtained by the statistical analyses of collected data: NW–SE and WSW–ENE, both of them with dip values higher than 70° (Fig. 9b). Calcite-filled veins are dominant in systematic sets, showing variable spacing ranging from several metres down to 30–40 cm. The vein walls are both undulating and steeped; the aperture is from few centimetres up to 15 cm. Spatic and globular calcite cements the discontinuities. Westward dipping, N–S striking faults have pluri-metric spacing within the fracture carbonates. Faults show planar to curvilinear surfaces entirely covered by calcite concretions. When clearly observed, normal kinematics has been detected for these faults. It is worth nothing that the veins systematically
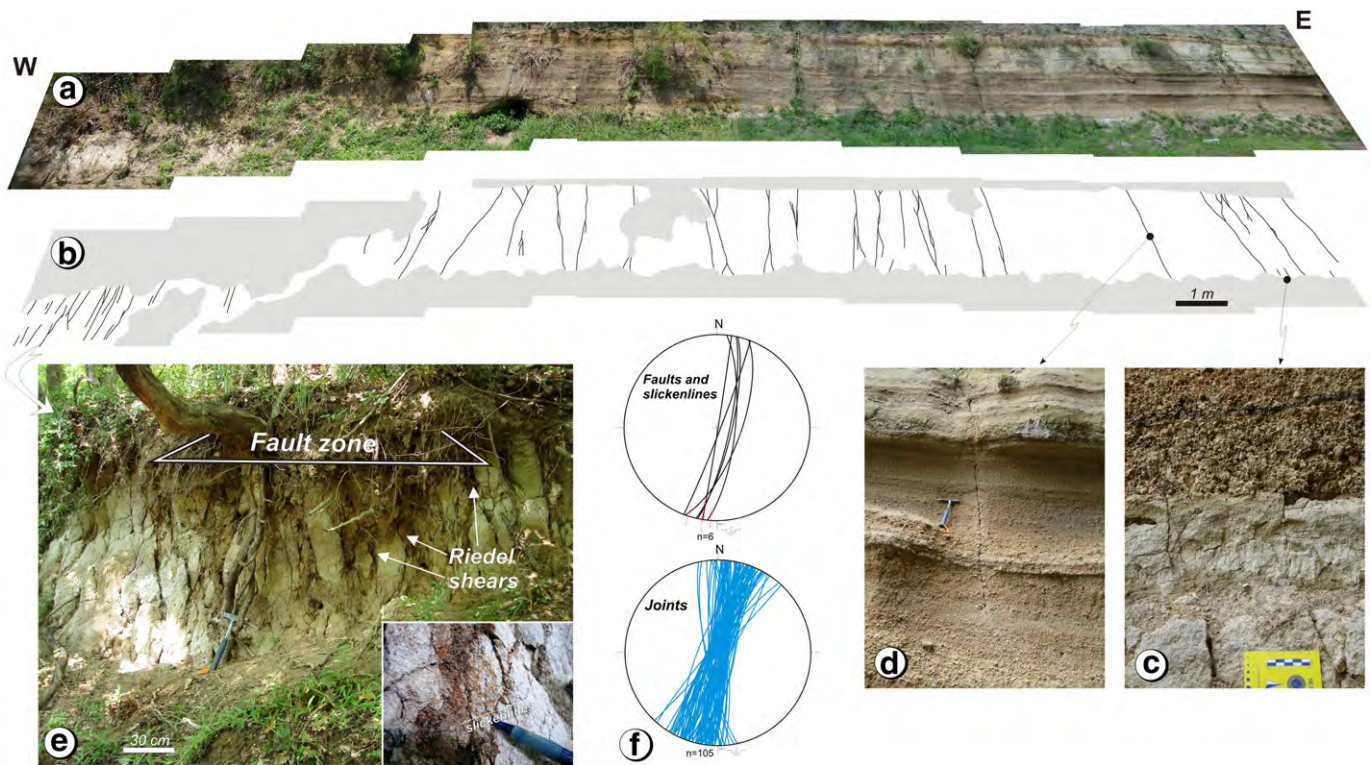
Fig. 5. (a) Panoramic view and (b) line drawing of fault array detected in pyroclastites (volcanic units; structural stop no. 14); (c) shear fractures in dense cineritic layers do not cross the overlying clastic one; (d) metric-persistence fracture accommodating pyroclastic layering; (e) dextral strike-slip fault damage zone cross-cutting all the volcanic sequence (the insert details the slickenlines detected on the fault surface); (f) stereographic projections (Schmidt net, lower hemisphere) showing that all the measured features are disposed NNE–SSW.

interrupt against the fault surfaces and the vein mineralisation deposited along the fault walls (Fig. 10c). Within wider veins, spatic calcite develops along the vein walls, while the internal portion is entirely filled by travertine concretions (Fig. 10d). At the mesoscale, calcite-filled veins show heterogeneous internal texture (Fig. 10e) defined by different domains with different colours (from white to light brown) corresponding to a change in chemical properties of the depositional fluid. These domains are representative of the sequential pulses of carbonate deposition during vein growth. The evidence of multiple generation of carbonate mineralisation in the area is also represented by the occurrence of 3–4 cm thick carbonatic concretion with irregular geometry that grows as an epidermal concretion sealing the above mentioned fracture network (Fig. 10f).

Vein systems have been also observed in travertine deposits occurring northern of the San Casciano dei Bagni village. Veins have variable width (from few centimetres up to 60 cm), metric spacing, and they strike along NE–SW direction. Within the massive travertine a half metre thick paleosol occurs (Fig. 10g) as individuating a standstill during the travertine deposition.

4. Geochronology

In the present work we have dated, using U-series disequilibrium method, two calcite-filled veins from the Mesozoic limestone of the Tuscan series, located north of the San Casciano dei Bagni Village (Fig. 9a). Three samples have been selected, representative of (i) two different generations of calcite-filled veins (samples CV1 and CV2), (ii) the speleothem sealing the fracture network (sample FL1), and (iii) the travertine resting below the paleosol (sample TR1).

Table 1 reports uranium contents, activity ratios and the ages of the dated samples. The ages for samples CV1, CV2, and FL1 have been obtained using a single sample, without using any correction model. These carbonates, in fact, are not contaminated with a detrital fraction

as can be inferred by a $^{230}Th/^{232}Th$ activity ratio higher than 80. The $^{230}Th/^{234}U$ ratio and the uranium content systematically decrease passing from sample CV1 to CV2, to FL1. Sample CV1 (large vein) gives age of 212 +53/−37 ky; sample CV2 (thin vein intruded within CV1) gives age of 120 ± 15 ky. The epidermal speleothem gives younger age of 95 ± 10 ky.

The travertine sample (TR1) is quite contaminated with a detrital fraction as can be inferred by a $^{230}Th/^{232}Th$ activity ratio ranging around 4 (Table 1), a value indicating the presence of a moderate amount of ^{232}Th accompanied by ^{230}Th not formed by radioactive decay of co-precipitated U in the carbonate fraction. The detrital ^{230}Th biases the $^{230}Th/^{234}U$ activity ratio of the pure carbonate fraction and thus the calculated age of the travertine, and therefore needs to be corrected. We used the "crustal correction model" with the assumption that all detrital Th have an average upper crustal $^{230}Th/^{232}Th$ activity ratio of 0.85 ± 0.36 (Wedepohl, 1995). This sample gives age of 182 +47/−35 ky.

5. Lineament analysis

Through the lineament analysis we focused on the identification of the main morphostructural and structural lineament patterns that characterise the area, aiming at inferring the role of fracturing and secondary permeability at the different scales, as well as to generalise the data acquired during the field survey. While some of these lineaments could be clearly identified as faults and other known structural features directly observed in the field, most of the others could not be associated with visible feature on the field. These morphological lineaments match with the alignment of valleys, borders of valleys, ridges or, preferably, combinations of these features and they cluster as groups with similar azimuths and well defined regions. These groups (lineament domains) are proved to be related to the recent stress conditions in the upper crust (Wise et al., 1985), and may provide useful information for describing the general fracturing and faulting pattern.
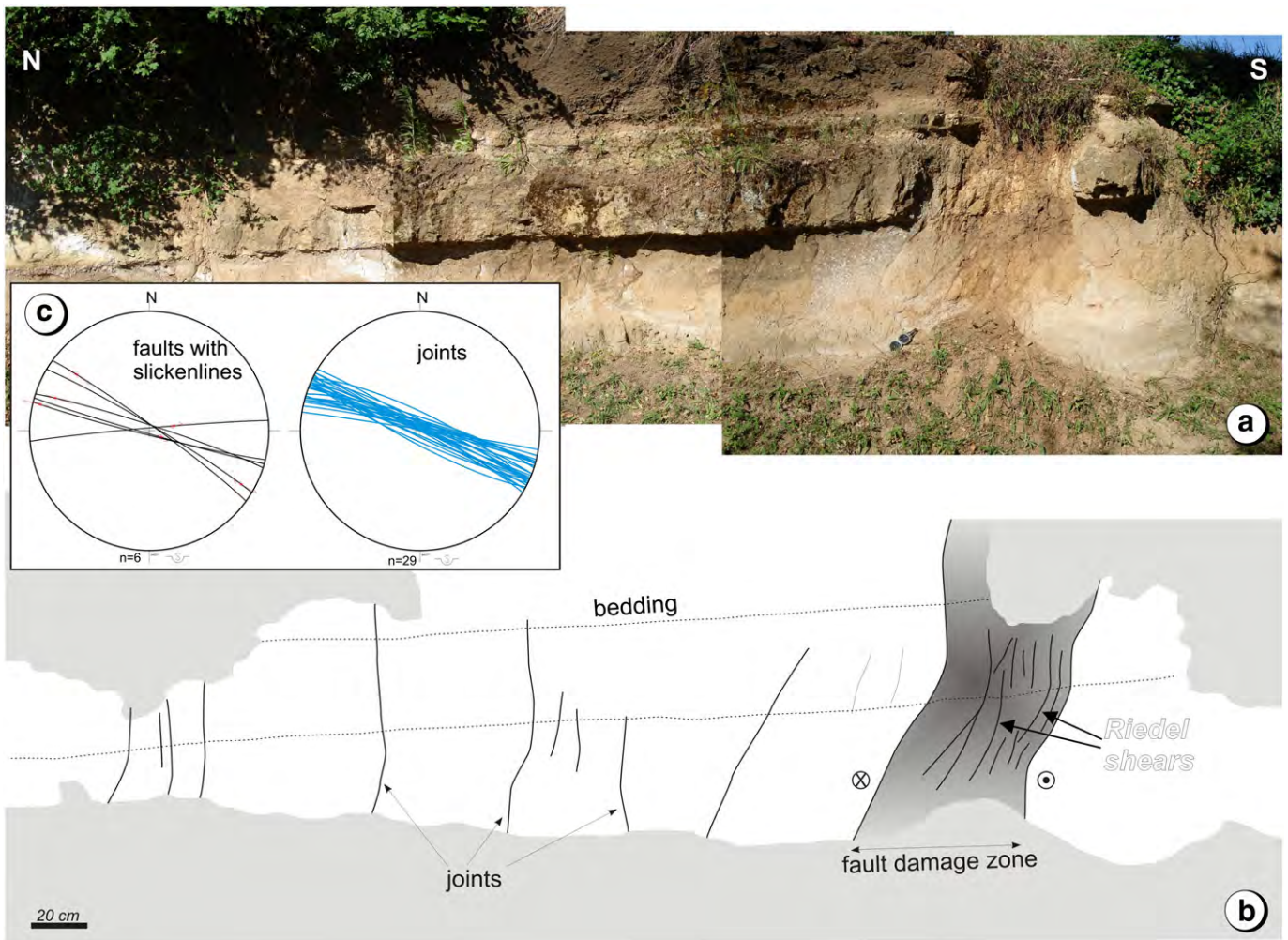
Fig. 6. (a) Panoramic view and (b) line drawing of fault array detected in pyroclastites (volcanic units; structural stop no. 23) producing metric damage zone and associated fracture system; (c) stereographic projections (Schmidt net, lower hemisphere) showing that all the measured features are disposed WNW–ESE.

Analysis was carried out on two different Digital Elevation Models (DEMs) with 60 m (SRTM, http://www2.jpl.nasa.gov/srtm/srtmBibliography.html) and 15 m (ASTER Gdem, http://asterweb.jpl.nasa.gov/gdem.asp) of spatial resolution, in order to perform a regional and a local detection of lineaments. Analysis of regional lineaments on the 60 m spatial resolution DEM identified 8359 features based on 8 shaded-relief models (Fig. 11a). Lineaments have lengths between 400 m and 8 km (with 1600–1800 m as a mean). Two main directions (NE–SW and NW–SE) and two subordinate directions (N–S and E–W) have been determined (Fig. 11b). Analysis of lineaments on a 15 m spatial resolution DEM allowed the grouping 4453 features along two main directions (NE–SW and NW–SE) and one minor direction (N–S). The lengths of these segments range between 200 m and 4 km (with a mean of 900–1000 m). The trend distribution and density of the lineaments have been considered also in relationship with the lithostratigraphic units in outcrop (volcanic deposits, Pliocene–Quaternary marine sediments, and allochthonous flysch; Fig. 11c). The area covered by volcanic rocks is characterised by the occurrence of 657 lineaments (15 m DEM) aligned along NW–SE and NNE–SSW main directions. The N–S and NE–SW directions are subordinate. The length of lineaments ranges between 200 m and 3 km. Longer features are concentrated along the NNE–SSW direction.

A map of the density of the lineaments (km/km^2) identified on the 15 m spatial resolution DEM is shown in Fig. 12: the length of a part of lineament that falls within a km-radius circular area around each pixel of the image is multiplied by the entire length of the same lineament. Values obtained for each lineament included in that circular area are cumulated and divided by the circle area. The base-map shows the density of all the lineaments, while contours highlight the difference between the density distributions of each family of orientation direction. In general, maximum values of density (22–25 km/km^2) are concentrated in the south-western part of the study area, and near the productive wells (8–11 km/km^2).

The contouring emphasises that the area on top of the structural high of Torre Alfina corresponds to an area of high density lineament, selectively affected by dominantly NNW-trending lineaments and intersecting NNE- and NE-trending lineaments. Values of density for each one of those group of lineaments reach a maximum of 4000 m/km^2. Productive wells (A1bis, A7, A13) are located in correspondence of intersections between lineament groups. The RA1 productive well is within a high density lineament area where NE-trending lineaments intersect NNW-trending ones. The A5 and A4 unproductive wells fall in low lineament density areas. The A14 well is in a high density area characterised by NE-trending lineaments, and this defines a significant difference to the area where productive ones are located. The A14 well is in fact located at the northern edge of the Bolsena structural caldera rim where volcano-tectonic lineaments are dominant. The A2 unproductive well falls at the southern edge of the high density area
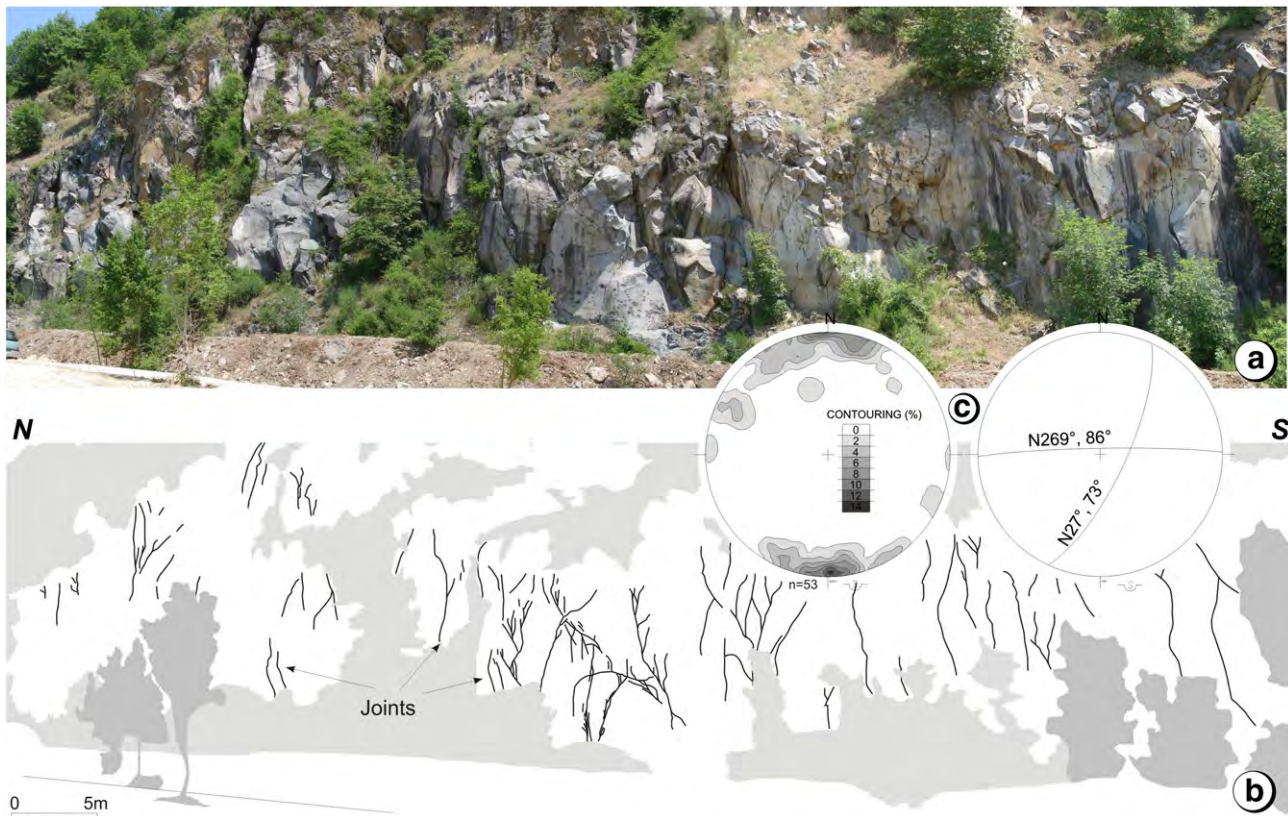
Fig. 7. (a) Panoramic view and (b) line drawing of joint systems detected in lavas (volcanic units; structural stop no. 5); (c) stereographic projections (Schmidt net, lower hemisphere) showing that the measured features are disposed in NNE–SSW and E–W orientations.

on the structural high of Torre Alfina. With respect to the productive wells, the location of A2 well does not overlap intersections between NNW- and NE-trending lineaments.

Other areas of concentration of higher density of lineaments occur in the south-western and north-western areas, where mainly NNE–SSW and NE–SW lineaments cross-cut each other reaching 8/10 km/km².

6. Discussion

6.1. The role of tectonic deformation at the Torre Alfina–Mount Cetona area

Geometrical relations provided by the stacking of Jurassic–Cretaceous carbonates on top of the flysch sequence induce to re-consider the Mount Cetona as a tectonic ridge positioned at an upper structural level with respect to the carbonate reservoir at the Torre Alfina area. Consequently, it is difficult to claim a hydraulic continuity between the overturned anticline of the Mount Cetona and the thrust stacking below the Torre Alfina area (as imaged by the stratigraphy of the Alfina 15 well). In this view, the allochthonous flysch constitutes (i) the sole thrust of the Tuscan series at the Mount Cetona and (ii) the roof thrust of the carbonatic reservoir at the Torre Alfina area. This structural arrangement can be explained considering the Mount Cetona as internal (i.e. westernmost) sheet (see also Buonasorte et al., 1987b) imbricated in out-of-sequence thrusting propagation during the Tertiary fold-and-thrust tectonics in the central Apennines. In this view, a structural discontinuity should exist between the Mount Cetona and the Torre Alfina reservoir. The interposed flysch sequence forms a hundred metres thick aquiclude hampering the direct hydrological communication between two sectors.

Our structural data confirm that a tectonic activity developed during the post-orogenic phases in the central Apennines in areas corresponding to the geothermal field (the Torre Alfina area) and the Mount Cetona (with its southern culmination in the San Casciano dei Bagni). Brittle deformation structures in Torre Alfina, mainly consisting of fracturing and faulting, show consistent grouping along NE–SW and WNW–ESE main directions. Fault zones affecting both the volcanic cover and the seal units are similar in terms of geometry (attitude and spatial distribution) and kinematics (strike-slip-to-normal sense of motion). The collected structural data document a dominant NE–SW and a subordinate E–W as maximum extension directions. The occurrence of NW–SE- and WSW–ENE-striking extensional fractures associated with faulting in carbonates at Mount Cetona documents the tectonic deformation that disrupts and segments the anticline structure.

The consistence of the lineament analysis allows generalising to a regional scale the importance of the tectonic structures detected in the field. Although there is no clear one-to-one correspondence with specific faults mapped at the surface, these lineaments may include fault zones extending to depth and involving the overall geothermal system. By comparing the spatial distribution of geological features deduced by DEM analysis with the main directions of tectonic features measured on the field it is evident that NE–SW and WNW–ESE main alignments can be distinguished. These structures can be reconciled with fault systems controlling the sedimentary setting of the Radicofani and Paglia–Tevere grabens and the present-day geometry of the carbonate structural highs in the area. The surface pattern and the kinematics indicate that our fault systems are part of the Pliocene–Quaternary regional extensional episode involving the Tyrrhenian margin of the central Italy (e.g. Brogi, 2008; Brogi et al., 2012; Buonasorte et al., 1988; Carmignani et al., 1994; Faccenna et al., 1994a, 1994b; Liotta et al., 2010; Rossetti et al., 2011), in which the strike-slip kinematics adjusts the block arrangement and transfers the deformation between the main normal-sense shear zones (Acocella and Funiciello, 2006). The present activity of strike-slip
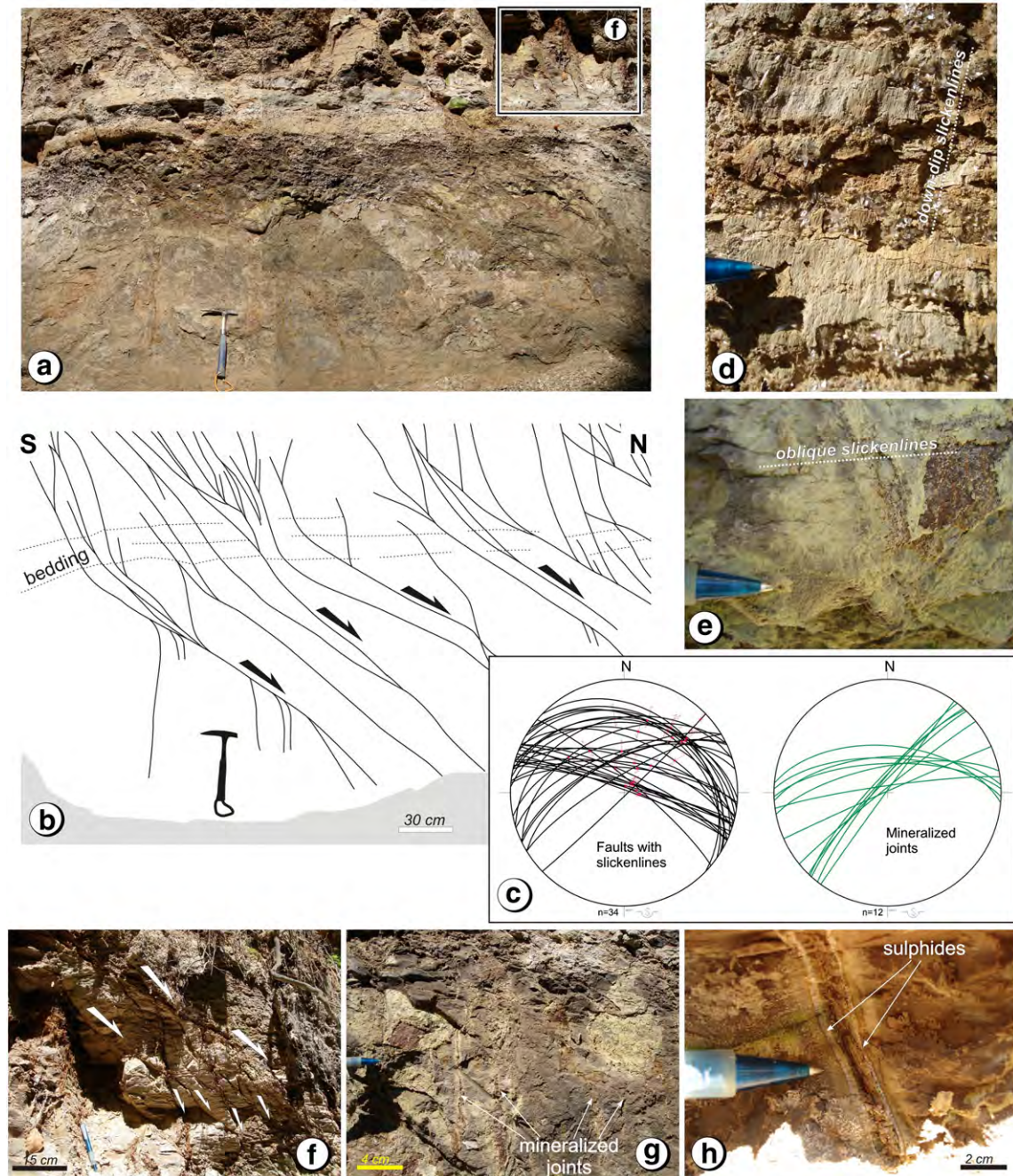
Fig. 8. (a) Panoramic view and (b) line drawing of fault array detected in Ligurian units (structural stop no. 17); (c) stereographic projections (Schmidt net, lower hemisphere) of the collected data; (d) detail of the down-dip slickenlines detected on the fault surfaces; (e) detail of the along strike slickenlines detected on the fault surfaces; (f) zoom on fault architecture composed of curved splays with normal kinematics; (g) set of mineralized joint system occurring at the hanging-wall of the fault system, showing dilatation and sulphide rimming of the joint walls.

and normal-sense tectonics is confirmed by the seismicity and focal mechanisms collected for the area (Fig. 2a), suggesting that present tectonic deformation in the Torre Alfina area is localising at the margin of the maximum convergence of geothermal flux, approximately where main post-orogenic fault zones are localised.

6.2. Tectonic structures and the hydrodynamic network of the endogenous fluids

The investigated area is part of a regional geothermal–hydrothermal domain that captured the interest of industries and researchers. The role of tectonic structures on the hydrothermal circulation in central

Apennines has been documented for areas characterised by geothermal pulses (e.g. Annunziatellis et al., 2008; Brogi, 2008; Rossetti et al., 2011) and travertine deposition (e.g. Faccenna et al., 1994b, 2008; Brogi et al., 2010, 2012; Gasparrini et al., 2013; Minissale et al., 2002), promoting inspiring insights for geothermal studies.

It is widely demonstrated that major tectonic cracks, where sufficiently interconnected, determine the hydraulic permeability within the rock volume, and that the fluid pressure gradients induce movements of fluids into and along the discontinuities until they are sealed (Cox et al., 2001; Rowland and Sibson, 2004; Sheldon and Ord, 2005; Sibson, 2000). In these conditions, fluid flow passes from pervasive (i.e. infiltrating isotropically the rock volume along the grain boundaries and
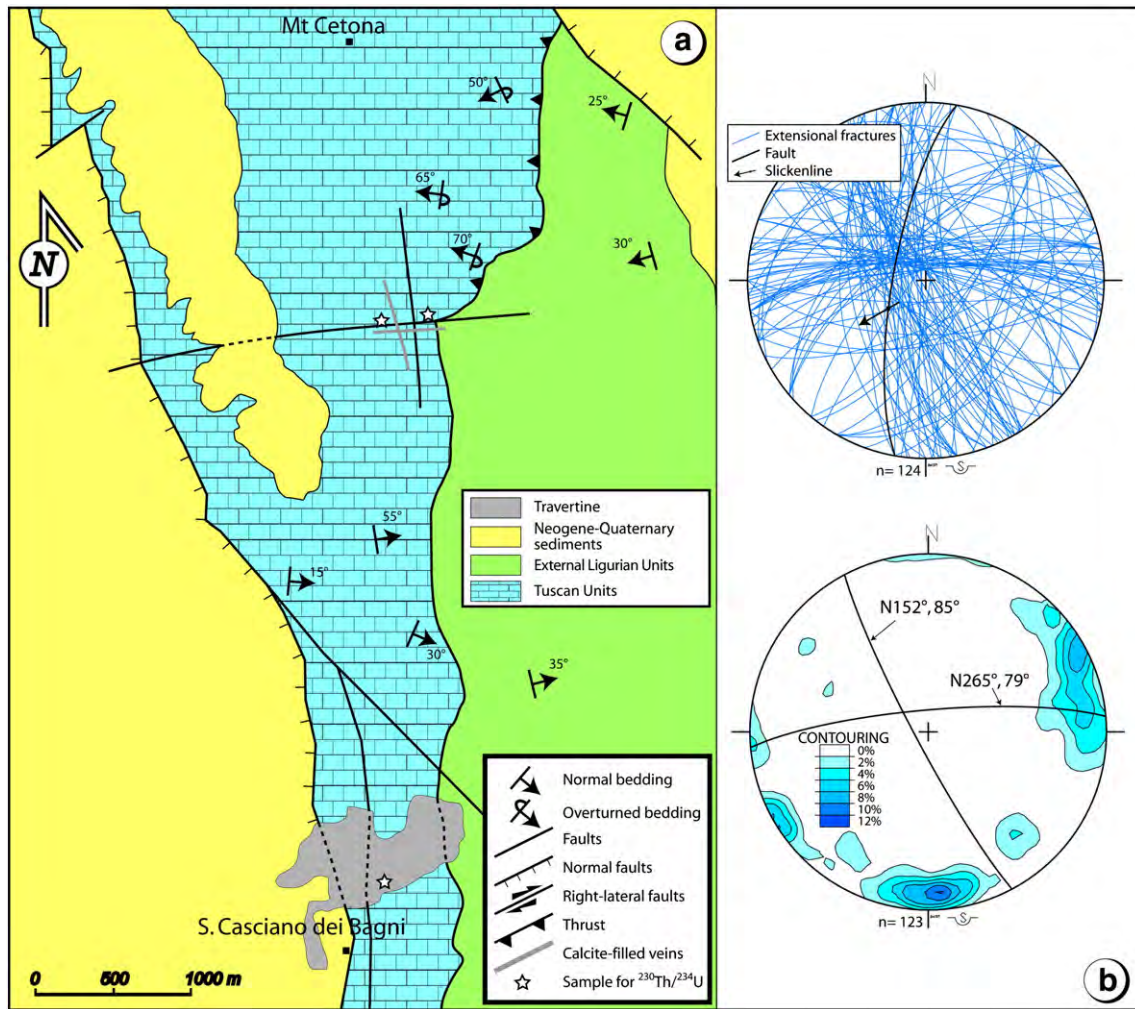
Fig. 9. (a) Structural map of the San Casciano dei Bagni area; (b) stereographic projections (Schmidt net, lower hemisphere) and contouring of the data collected in the San Casciano dei Bagni area, suggesting two main tectonic directions (NNW–SSE and E–W).

microcracks) to channelized. Several studies document channelisation of fluids within the geothermal systems in correspondence of deformation zones, and consequent fluid discharge along fluid pathways has a primary role for the escape of endogenous gases at the surface (e.g. Azzaro et al., 1998; Chiodini et al., 2007; Etiope et al., 1999; Kaven et al., 2011; Khomsi et al., 2012). It has been also demonstrated that deformation zones may also act as hydraulic barriers to fluid flow (e.g. Faulkner and Rutter, 2001), as effect of rock comminution during fault slip or secondary mineralisation.

According to these concepts, we can address the superficial geothermal manifestations in the Torre Alfina area to the activity of the tectonic structures.

1. In the Cetona ridge, the localisation of heterogeneous hydrochemical and isotopic compositions of spring waters (Piscopo et al., 2009) shows that the structural setting controls fluid circulation. Dominant cold calcium–bicarbonate waters of meteoric origin are abundant within the Cetona ridge, while dominant hot calcium–sulphate waters spring-out in the area of San Casciano dei Bagni, in association with travertine deposition. This evidences two distinct groundwater circulation circuits in the Mount Cetona area, which have different recharge systems and are not in hydraulic connection. This suggests that the documented deformation structures that occur between Mount Cetona and San Casciano dei Bagni (Fig. 9) act as an impermeable barrier to horizontal fluid migrations.

2. Faulting and fracturing at Cetona–San Casciano dei Bagni area are associated with intense hydrothermal manifestations and travertine deposition. $^{230}Th/^{234}U$ dating allows distinguishing three different stages of hydrothermal pulses represented by (i) calcite deposition and self-sealing of fault-related fractures in systematic sets (at about 200 ka), (ii) crystallisation of spatic and globular calcite that is more common in non-systematic sets (at about 120 ka), and (iii) the late speleothem (95 ka). A cyclic interplay between the activity of tectonic structures (fault-fracture permeability in the rock volume), the shear stress, and the fluid pressure within the fluid-rock system (e.g. Sibson, 2001) can be a plausible scenario for framing the relationships between hydrothermal circulation, travertine deposition and tectonic activity at San Casciano dei Bagni. Accordingly, fluid mineralisation in the study area provides evidence for hydrothermal circulation in the reservoir units.

3. The anomalous geothermal gradient (1.7–2.1 °C/10 m measured within the volcanic sediments; Buonasorte et al., 1988) results to be confined in the area where geophysical and seismic data identified the buried structural high. An abrupt drop of the geothermal gradient (down to 0.6 °C/10 m) moving away from the structural high reveals the inefficiency of the flow to permeate horizontally and to distribute uniformly in the geothermal area. It is plausible to assume that post-orogenic deformation individuates preferential directions (NE–SW and WNW–ESE) along which fluids circulate through the reservoir. By considering the consistence of our dataset and following insights
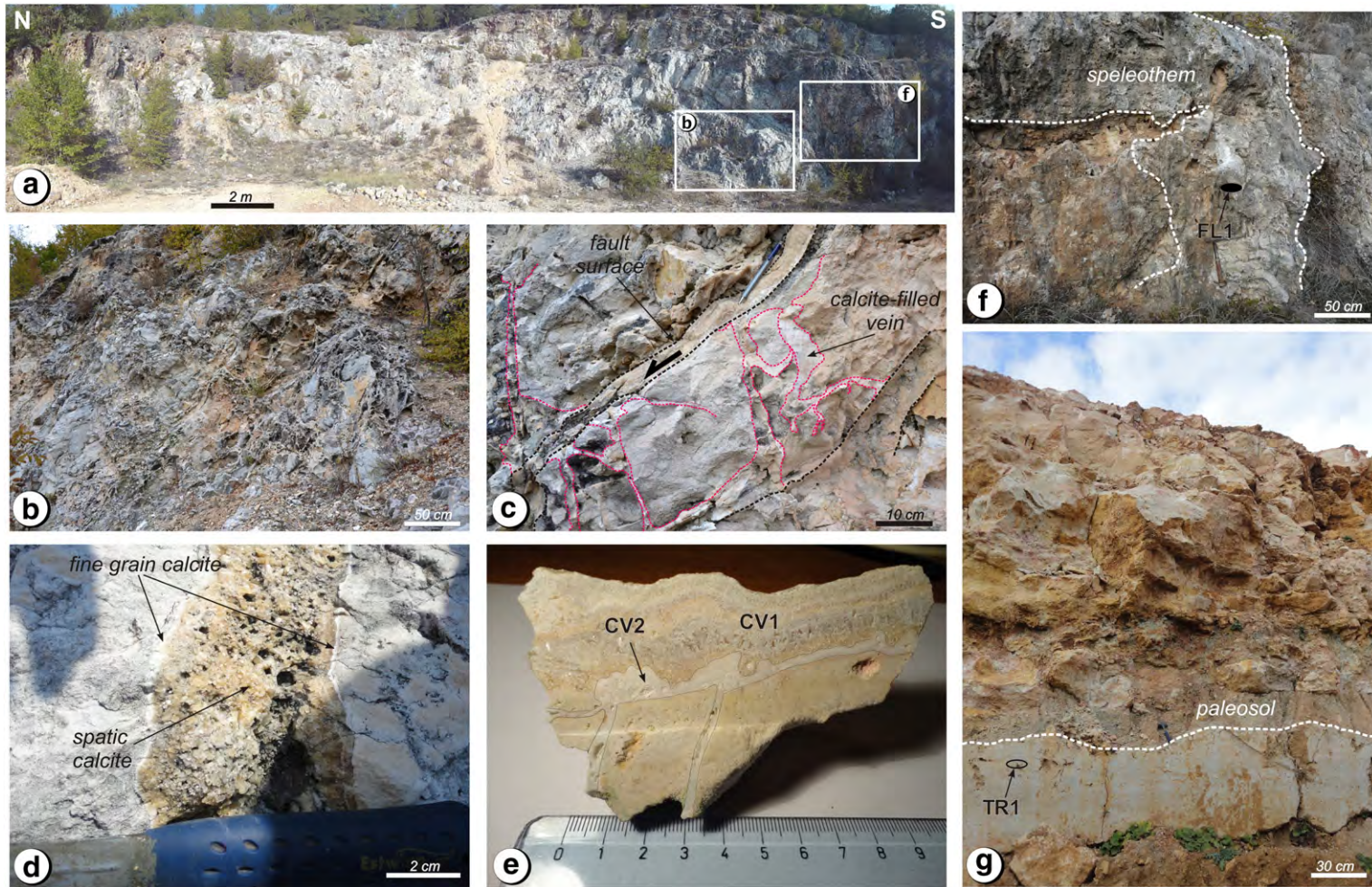
Fig. 10. (a) Panoramic view of the investigated area (the Saccaia Valley) where Tuscan units are affected by intense extensional fractures; (b) non-systematic set of calcite-filled veins; (c) detail of relationships between vein system and fault surface sealed by calcite crystallisation; (d) example of composite crystallisation in vein; (e) mesoscopic sample showing two different generations of vein formation, and used for the ^{230}Th/^{234}U dating method; (f) speleothem sealing the vein network and used for dating; (g) panoramic view of travertine cliff in quarry area near San Casciano dei Bagni; a paleosol is visible in between the travertine succession. The travertine below the paleosol has been sampled for the ^{230}Th/^{234}U dating method.

Table 1
Activity ratios, uranium concentrations and ages of two calcites in veins (CV1, CV2), the speleothem (FL1), and the travertine (TR1) outcropping near San Casciano dei Bagni Village. For the travertine sample, age has been corrected using crustal correction model.

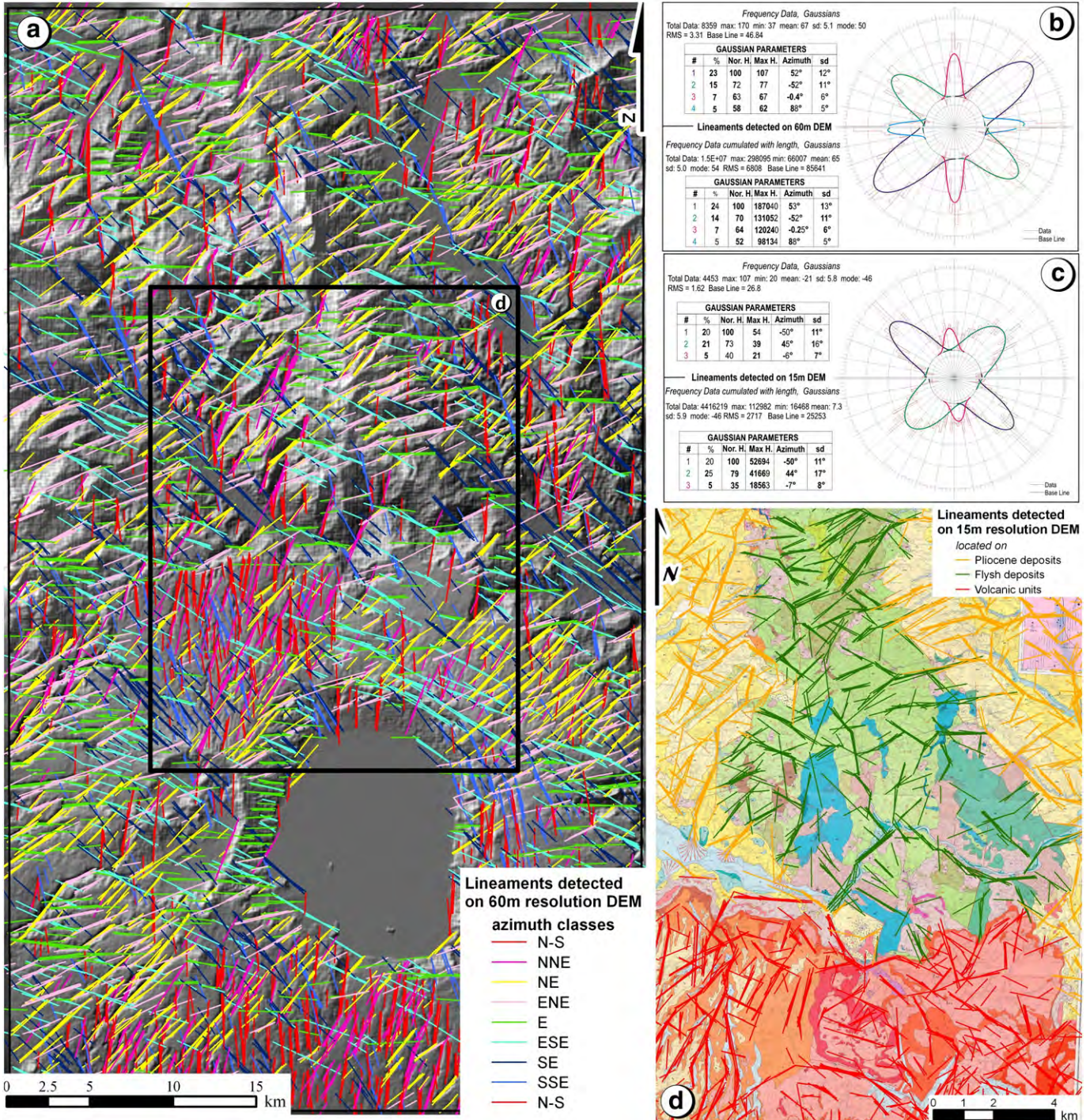| Sample	$^{230}Th/^{232}Th$	$^{230}Th/^{234}U$	$^{234}U/^{238}U$	U (ppm)	Corrected ($^{230}Th/^{234}U$)	Age (ky)
CV1	187 ± 29.631	0.85 ± 0.03	0.982 ± 0.031	0.063 ± 0.002		212 + 53/−37
CV2	86.454 ± 10.758	0.676 ± 0.047	1.081 ± 0.052	0.038 ± 0.001		120 ± 15
FL1	154.095 ± 19.531	0.585 ± 0.039	1.062 ± 0.057	0.028 ± 0.0012		95 ± 10
TR1	4.482 ± 0.315	0.871 ± 0.052	1.219 ± 0.041	0.031 ± 0.002	0.844 ± 0.074	182 + 47/−35

Fig. 11. (a) Map of regional lineaments on the 60 m spatial resolution DEM showing the different classes of lineament orientations; (b) rose diagram showing the spatial distribution of lineaments on the 60 m spatial resolution DEM; (c) rose diagram showing the spatial distribution of lineaments on the 15 m spatial resolution DEM; (d) distribution of the detected morphological lineaments on the geological map of the Torre Alfina area (Costantini et al., 1984). Colour legend: green_allochthonous flysch; yellow_Plio-Quaternary sediments; red_volcanics.
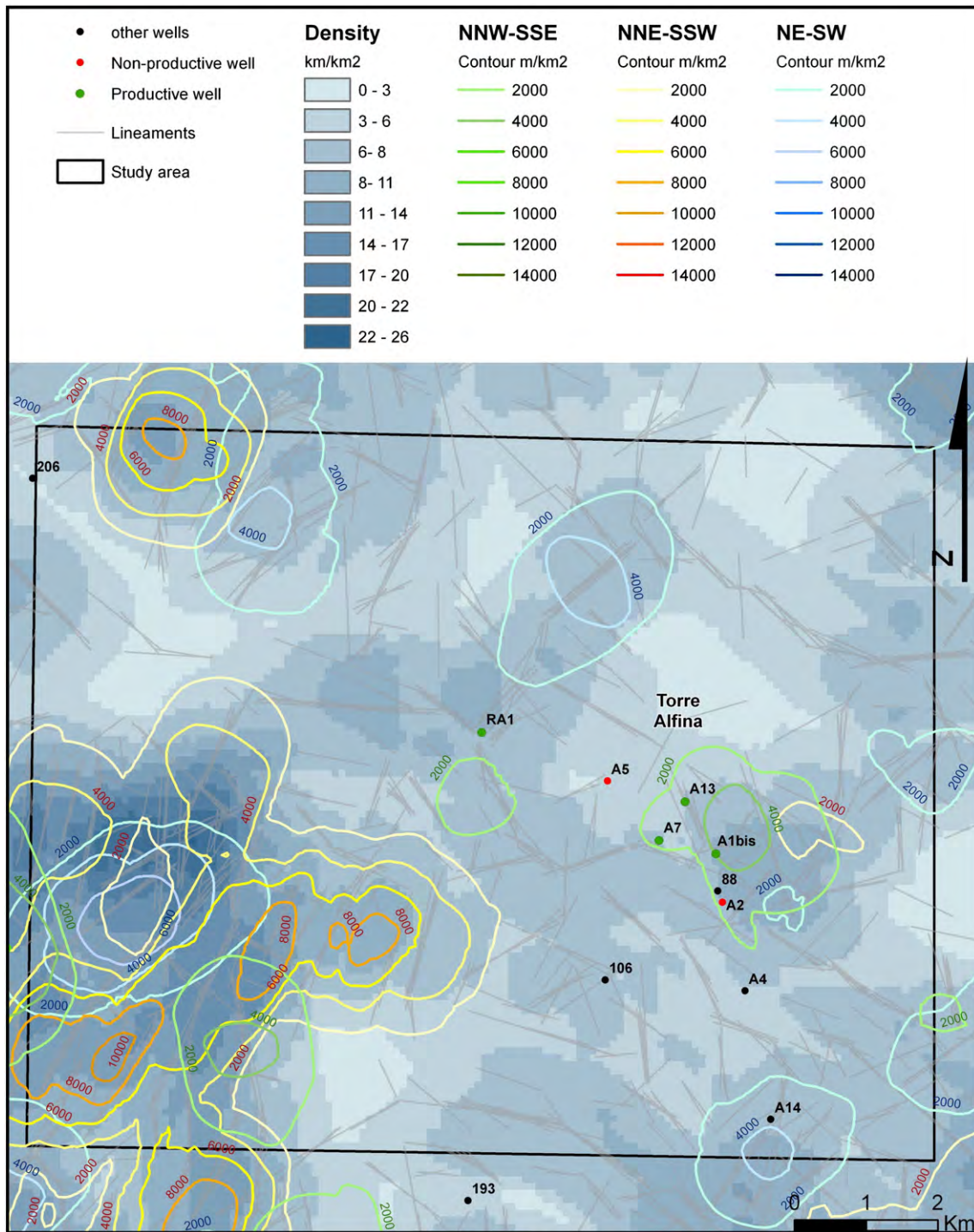
Fig. 12. Density map of lineaments and contouring grouped by orientation.

from numerical models for fluid convection (e.g. McLellan et al., 2010; Oliver et al., 2006), we assume that tectonic discontinuities in Torre Alfina area may have a double role: (i) as main paths of fluids in vertical sense, connecting different structural levels of the geothermal rock system and favouring the advection flow; and (ii) as main barriers for the horizontal motion of fluids, disconnecting the circulation at the same structural level. These features argue for a largely heterogeneous secondary permeability in a compartmentalised reservoir. The occurrence of randomly unproductive or very productive deep bore-holes within the same reservoir should be explained in these terms.

With the aim to delineate the role of tectonic structures and the compartmentalisation in the Torre Alfina geothermal system, we propose a 3D-view (Fig. 13), based on the model of Buonasorte et al. (1988). The present-day structural setting of the geothermal system consists of the interplay between structures related to the assemblage of the reservoir-seal system (i.e. during syn-orogenic phases) and structures dissecting the reservoir (i.e. activated during the post-orogenic phases and still active). In particular, we should address to the Tertiary fold-and-thrust tectonics in the central Apennines the construction of the duplex structures in the reservoir suitable for accumulating endogenous flux and the placement of the seal units. Then, the post-orogenic structures have
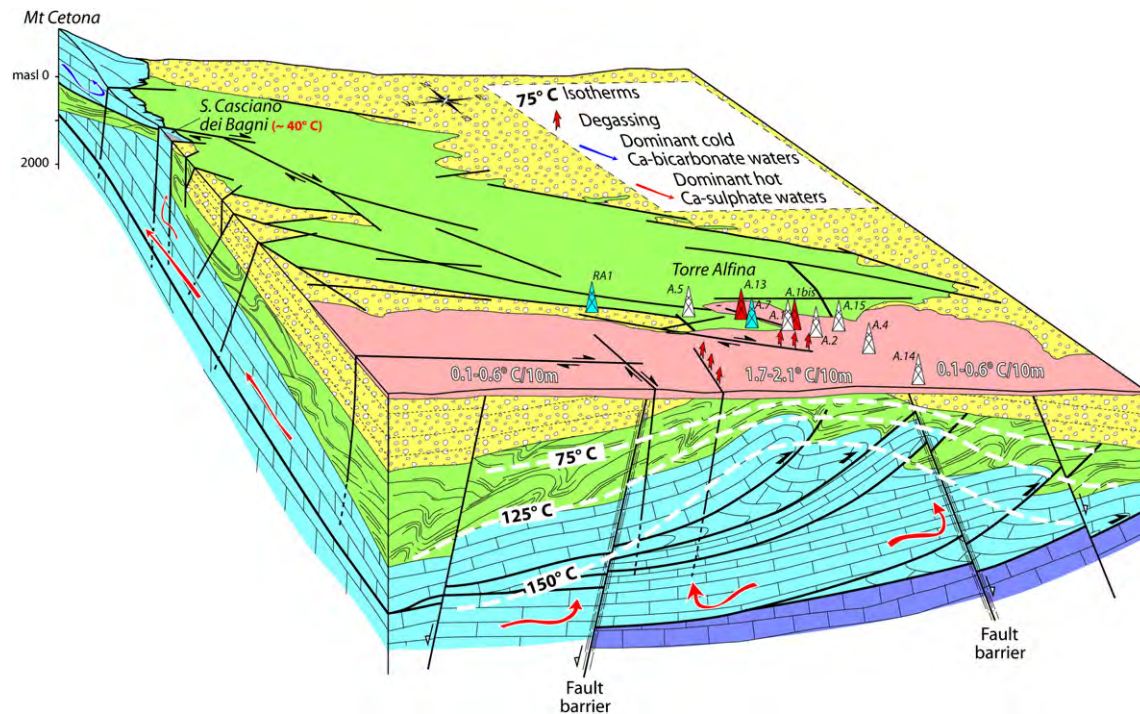
Fig. 13. 3D-block diagram re-interpreting the model by Buonasorte et al. (1988) on the light of the new dataset. Fault systems and related fracturation have primary role in controlling the underground fluid circulation and surface manifestations (as gas emission). The fault architecture is only indicative.

a primary role in controlling the geometric relationships between the main features of the geothermal system (reservoir, seal units, and recharge area) and the present-day fluid flow throughout the reservoir rock volume.

Defining the recharge area of the Torre Alfina geothermal system requires integration of multiple geological and geophysical techniques. However, the recognised structural discontinuity with the Mount Cetona reinforces the importance of the N–S-trending structural high connecting Torre Alfina with the Bolsena caldera as a plausible setting of hot fluids circulation (Fig. 2b).

7. Conclusions

Torre Alfina represents a key area for studying the effect of the tectonic deformation and its role on the geothermal system. Distribution, persistence, and geometry of the tectonic structures affect the fluid flow within the Torre Alfina geothermal system that can be imaged as composed of different compartments with inhomogeneous fluid network. Tectonic structures define the main boundaries between compartments, helping the understanding of why productive and nonproductive wells were found in apparently similar structural settings within the Torre Alfina field. The obtained results would emphasise the importance of identifying and utilising at best the indirect evidence at surface of secondary permeability in the reservoirs applied at the reappraisal of the potential of a geothermal volcano system. In particular, our case suggests that:

(i) the assessment of post-orogenic brittle deformation affecting the younger lithologies cropping out in the geothermal field (i.e. the volcanic coverture) can be used for obtaining indirect information on deformation fabrics driving the circulation of the endogenous fluids within the buried seal-reservoir complex;

(ii) the study of deformation in the exposed reservoir units provides insights for modelling the hydraulic connection between the geothermal field and the presumable recharge area;

(iii) the identification of the main morphostructural and structural lineament patterns through the lineament analysis should support the data acquired during the field survey in order to generalise the role of fracturing and secondary permeability at the regional scale;

(iv) the occurrence of hydrothermal mineralisation (e.g. travertine deposits) may be used for assessing the fossil fluid circulation in the recharge area with implication on the present-day fluid pathways;

(v) an accurate interpretation of the geological model supports the identification of the geothermal potential of a natural site, minimising failures both in the exploration and exploitation stages.

Appendix A.1. Geochronology

The ^{230}Th/^{234}U method is the most widely used dating technique applied to carbonates and is based on the extreme fractionation of the parent isotopes ^{238}U and ^{234}U from their long-lived daughter ^{230}Th in the hydrosphere. Uranium, markedly more soluble than Th in the surface and near-surface environments, is readily mobilized as the highly soluble uranyl ion (UO_2^{2+}) and its complexes, whereas Th is easily hydrolyzed and precipitated or adsorbed on detrital particles. Uranium is co-precipitated with $CaCO_3$ on exsolution of CO_2, while Th is generally negligible. In the absence of detrital Th, ^{230}Th only forms in situ by

radioactive decay of co-precipitated U. In a closed system the extent to which the $^{230}Th/^{234}U$ activity ratio has returned towards unity is a function of time, taking into account also the state of disequilibrium between ^{234}U and ^{238}U usually higher than 1.

Samples were crushed and ultrasonically washed in deionized water. Fragments were checked with a stereoscopic microscope to discard any recrystallized portions. About 30 g of sample was dissolved in 1 N nitric acid and filtered to separate the leachates from the insoluble residue. Few millilitres of hydrogen peroxide was added to the leachate and heated at 100 °C in order to destroy organic matter. Isotopic complexes of uranium and thorium were extracted according to the procedure described in Edwards et al. (1986) and alpha-counted using high resolution ion implanted Ortec silicon surface barrier detectors.

The ages of all samples were calculated by means of Isoplot/Ex (version3.0), a plotting and regression programme designed by Ludwig (2003) for radiogenic-isotope data. Errors are always quoted as 1σ.

References

Acocella, V., Funiciello, R., 2006. Transverse systems along the extensional Tyrrhenian margin of central Italy and their influence on volcanism. Tectonics 25, TC2003. http://dx.doi.org/10.1029/2005TC001845.

Acocella, V., Rossetti, F., 2002. The role of extensional tectonics at different crustal levels on granite ascent and emplacement: an example from Tuscany (Italy). Tectonophysics 354, 71–83.

Annunziatellis, A., Beaubien, S.E., Bigi, S., Ciotoli, G., Coltella, M., Lombardi, S., 2008. Gas migration along fault systems and through the vadose zone in the Latera caldera (central Italy): implications for CO_2 geological storage. Int. J. Greenhouse Gas Control 2, 353–372.

Argnani, A., Savelli, C., 1999. Cenozoic volcanism and tectonics in the southern Tyrrhenian Sea: spacetime distribution and geodynamic significance. J. Geodyn. 27, 409–432.

Árnason, K., Eysteinsson, H., Hersir, G., 2010. Joint 1D inversion of TEM and MT data and 3D inversion of MT data in the Hengill area, SW Iceland. Geothermics 39, 13–34.

Atkinson, B.K., 1987. Introduction to fracture mechanics and its geophysical applications. In: Atkinson, B.K. (Ed.), Fracture Mechanics of Rock. Academic Press, London, pp. 1–26.

Azzaro, R., Branca, S., Giammanco, S., Gurrieri, S., Rasà, R., Valenza, M., 1998. New evidence for the form and extent of the Pernicana Fault System-Mt. Etna/from structural and soil–gas surveying. J. Volcanol. Geotherm. Res. 84, 143–152.

Barberi, F., Innocenti, F., Landi, P., Rossi, U., Saitta, M., Santacroce, R., Villa, I.M., 1984. The evolution of Latera caldera (central Italy) in the light of subsurface data. Bull. Volcanol. 47 (1), 125–141.

Barberi, F., Buonasorte, G., Cioni, R., Fiordelisi, A., Foresi, L., Iaccarino, S., Laurenzi, M.A., Sbrana, A., Vernia, L., Villa, I.M., 1994. Plio-Pleistocene geological evolution of the geothermal area of Tuscany and Latium. Mem. Descr. Carta Geol. Ital. 49, 77–133.

Barchi, M.R., De Feyter, A., Magnani, M.B., Minelli, G., Pialli, G., Sotera, M., 1998. Extensional tectonics in the Northern Apennines (Italy); evidence from the CROP 03 deep seismic reflection line. Mem. Soc. Geol. Ital. 52, 527–538.

Bellani, S., Brogi, A., Lazzarotto, A., Liotta, D., Ranalli, G., 2004. Heat flow, deep temperatures and extensional structures in the Larderello geothermal field (Italy). Constraints on geothermal fluid flow. J. Volcanol. Geoth. Res. 132, 15–29.

Bibby, H.M., Caldwell, T.G., Davey, F.J., Webb, T.H., 1995. Geophysical evidence on the structure of the Taupo Volcanic Zone and its hydrothermal circulation. J. Volcanol. Geotherm. Res. 68, 29–58.

Brogi, A., 2008. The structure of the Monte Amiata volcano-geothermal area (Northern Apennines, Italy): Neogene–Quaternary compression versus extension. Int. J. Earth Sci. 97, 677–703.

Brogi, A., Fabbrini, L., 2009. Extensional and strike-slip tectonics across the Monte Amiata–Monte Cetona transect (Northern Apennines, Italy) and seismotectonic implications. Tectonophysics 476, 195–209.

Brogi, A., Capezzuoli, E., Aqué, R., Branca, M., Voltaggio, M., 2010. Studying travertines for neotectonics investigations: Middle–Late Pleistocene syn-tectonic travertine deposition at Serre di Rapolano (Northern Apennines, Italy). Int. J. Earth Sci. 99, 1383–1398.

Brogi, A., Capezzuoli, E., Buracchi, E., Branca, M., 2012. Tectonic control on travertine and calcareous tufa deposition in a low-temperature geothermal system (Sarteano, Central Italy). J. Geol. Soc. Lond. 169, 461–476.

Buonasorte, G., Fiordelisi, A., Rossi, U., 1987a. Tectonic structures and geometric setting of the Vulsini Volcanic Complex. Period. Mineral. 56, 123–136.

Buonasorte, G., Fiordelisi, A., Pandeli, E., Rossi, U., Sollevanti, F., 1987b. Stratigraphic correlation and structural setting of the pre-neoautochthonous sequences of Northern Latium. Period. Mineral. 56, 111–112.

Buonasorte, G., Cataldi, R., Ceccarelli, A., Costantini, A., D'Offizi, S., Lazzarotto, A., Ridolfi, A., Baldi, P., Barelli, A., Bertini, G., Bertrami, R., Calamai, A., Cameli, G., Corsi, R., D'Acquino, C., Fiordelisi, A., Gezzo, A., Lovari, F., 1988. Ricerca ed esplorazione nell'area geotermica di Torre Alfina (Lazio–Umbria). Boll. Soc. Geol. Ital. 107, 265–337.

Buonasorte, G., Pandeli, E., Fiordalisi, A., 1991. The Alfina 15 well: deep geological data from northern Latium (Torre Alfina geothermal area). Boll. Soc. Geol. Ital. 110, 823–831.

Caine, J.S., Evans, J.P., Forster, C.B., 1996. Fault zone architecture and permeability structure. Geology 24, 1025–1028.

Carmignani L. and Lazzarotto A (Coordinators), 2004. Geological map of Tuscany (Italy). Available at http://www.egeo.unisi.it/.

Carmignani, L., Decandia, F.A., Disperati, L., Fantozzi, P.L., Lazzarotto, A., Liotta, D., Meccheri, M., 1994. Tertiary extensional tectonics in Tuscany (Northern Apennines Italy). Tectonophysics 238, 295–315.

Cas, R.A.F., Giordano, G., Esposito, A., Balsamo, F., Lo, Mastro S., 2011. Hydrothermal breccia textures and processes: Lisca Bianca Islet, Panarea, Eolian Islands, Italy. Econ. Geol. 106, 437–450.

Chiarabba, C., Amato, A., Fiordelisi, A., 1995. Upper crustal tomographic images of the Amiata–Vulsini geothermal region, central Italy. J. Geophys. Res. 100, 4053–4066.

Chiodini, G., Frondini, F., Ponziani, F., 1995. Deep structures and carbon dioxide degassing in Central Italy. Geothermics 24, 81–94.

Chiodini, G., Baldini, A., Barberi, F., Carapezza, M.L., Cardellini, C., Frondini, F., Granirei, D., Ranaldi, M., 2007. Carbon dioxide degassing at Latera caldera (Italy): evidence of geothermal reservoir and evaluation of its potential energy. J. Geophys. Res. 112, B12204. http://dx.doi.org/10.1029/2006JB004896.

Costantini, A., Ghezzo, C., Lazzarotto, A., 1984. Carta geologica dell'area geotermica di Torre Alfina (prov. Di Siena-Viterbo-Terni). ENEL, Unità Nazionale Geotermica, Pisa (Cartografia S.EL.C.A., Firenze).

Cox, S.F., Knackstedt, M.A., Braun, J., 2001. Principles of structural controls on permeability and fluid flow in hydrothermal systems. Rev. Econ. Geol. 14, 1–24.

Doveri, M., Lelli, M., Marini, L., Raco, B., 2010. Revision, calibration and application of the volume method to evaluate the geothermal potential of some recent volcanic areas of Latium, Italy. Geothermics 39, 260–269.

Edwards, R.L., Chen, J.H., Wasseburg, G.J., 1986. $^{238}U–^{234}U–^{230}Th–^{232}Th$ systematics and the precise measurement of time over the past 500000 years. Earth Planet. Sci. Lett. 81, 175–192.

Etiope, G., Beneduce, P., Calcara, M., Favali, P., Frugoni, F., Schiattarella, M., Smriglio, G., 1999. Structural pattern and $CO_2–CH_4$ degassing of Ustica Island, Southern Tyrrhenian basin. J. Volcanol. Geotherm. Res. 88, 291–304.

Faccenna, C., Funiciello, R., Bruni, A., Mattei, M., Sagnotti, L., 1994a. Evolution of a transfer related basin: the Ardea basin (Latium, Central Italy). Basin Res. 5, 1–11.

Faccenna, C., Funiciello, R., Mattei, M., 1994b. Late Pleistocene N–S shear zones along the Latium Tyrrhenian margin: structural characters and volcanological implications. Boll. Geofis. Teor. Appl. 36, 507–522.

Faccenna, C., Mattei, M., Funiciello, R., Jolivet, L., 1997. Styles of back-arc extension in the Central Mediterranean. Terra Nova 9, 126–130.

Faccenna, C., Soligo, M., Billi, A., De Filippis, L., Funiciello, R., Rossetti, C., Tuccimei, P., 2008. Late Pleistocene depositional cycles of the Lapis Tiburtinus travertine (Tivoli, central Italy): possible influence of climate and fault activity. Glob. Planet. Chang. 63, 299–308. http://dx.doi.org/10.1016/J.Gloplacha.2008.06.006.

Faulkner, D.R., Rutter, E.H., 2001. Can the maintenance of overpressured fluids in large strike-slip fault zones explain their apparent weakness? Geology 29, 503–506.

Funiciello, R., Giordano, G. (Eds.), 2010. The Colli Albano Volcano. Special Publications of IAVCEI, 3. Geological Society, London (392 pp.).

Funiciello, R., Locardi, E., Parotto, M., 1976. Lineamenti geologici dell'area Sabatina orientale. Boll. Soc. Geol. Ital. 95, 831–849.

Gambardella, B., Cardellini, C., Chiodini, G., Frondini, F., Marini, L., Ottonello, G., Vetuschi, Zuccolini M., 2004. Fluxes of deep CO_2 in the volcanic areas of central-southern Italy. J. Volcanol. Geotherm. Res. 136, 31–52.

Garg, S.K., Pritchett, J.W., Wannamaker, P.E., Combs, J., 2007. Characterization of geothermal reservoirs with electrical surveys: Beowawe geothermal field. Geothermics 36, 487–517.

Gasparrini, M., Ruggieri, G., Brogi, A., 2013. Diagenesis versus hydrothermalism and fluid–rock interaction within the Tuscan Nappe of the Monte Amiata CO_2-rich geothermal area (Italy). Geofluids. http://dx.doi.org/10.1111/gfl.12025.

Giordano, G., De Benedetti, A.A., Diana, A., Diano, G., Gaudioso, F., Marasco, F., Miceli, M., Mollo, S., Cas, R.A.F., Funiciello, R., 2006. The Colli Albani mafic caldera (Roma, Italy): stratigraphy, structure and petrology. J. Volcanol. Geotherm. Res. 155, 49–80.

Giordano, G., Pinton, A., Cianfarra, P., Baez, W., Chiodi, A., Viramonte, J., Norini, G., Groppelli, G., 2012. Structural control on geothermal circulation in the Cerro Tuzgle–Tocomar geothermal volcanic area (Puna plateau, Argentina). J. Volcanol. Geotherm. Res. (ISSN: 0377-0273) 249, 77–94. http://dx.doi.org/10.1016/j.jvolgeores.2012.09.009.

Guillou-Frottier, L., Carrè, C., Bourgine, B., Bouchot, V., Genter, A., 2013. Structure of hydrothermal convection in the Upper Rhine Graben as inferred from corrected temperature data and basin-scale numerical models. J. Volcanol. Geotherm. Res. 256, 29–49.

Jolivet, L., Faccenna, C., Goffé, B., Mattei, M., Rossetti, F., Brunet, C., et al., 1998. Midcrustal shear zones in post-orogenic extension: example from the northern Tyrrhenian Sea (Italy). J. Geophys. Res. 103, 12123–12160.

Jousset, P., Haberland, C., Bauer, K., Arnason, K., 2011. Hengill geothermal volcanic complex (Iceland) characterized by integrated geophysical observations. Geothermics 40, 1–24.

Kastens, K., Mascle, J., Auroux, C.A., et al., 1988. ODP Leg 107 in the Tyrrhenian Sea: insights into passive margin and back-arc basin evolution. Geol. Soc. Am. Bull. 100, 1140–1156.

Kaven, J.O., Hickman, S.H., Davatzes, N.C., 2011. Micro-seismicity, fault structure and hydraulic compartmentalization within the Coso geothermal field, California. Proceedings, Thirty-sixth Workshop on Geothermal Reservoir Engineering, Stanford University, Stanford, California, January 31–February 2, 2011 SGP-TR-191 (8 pp.).

Khomsi, S., Echihi, O., Slimani, N., 2012. Structural control on the deep hydrogeological and geothermal aquifers related to the fractured Campanian–Miocene reservoirs of northeastern Tunisia foreland constrained by subsurface data. C. R. Geosci. 344, 247–265.

Liotta, D., 1994. Structural features of the Radicofani basin along the Piancastagnaio (Mt. Amiata)—S. Casciano dei Bagni (Mt. Cetona) cross section. Memor. Soc. Geol. Ital. 48, 401–408.

Liotta, D., Ruggieri, G., Brogi, A., Fulignati, P., Dini, A., Cardini, I., 2010. Migration of geothermal fluids in extensional terrains: the ore deposits of the Boccheggiano-Montieri area (southern Tuscany, Italy). Int. J. Earth Sci. 99, 623–644.

Ludwig, K.R., 2003. Using isoplot/Ex version 3. A geochronological toolkit for Microsoft Excel. Berkeley Geochronology Ctr. Spec. Pub., 4.

Malinverno, A., Ryan, W.B.F., 1986. Extension in the Tyrrhenian Sea and shortening in the Apennines as result of arc migration driven by sinking of the lithosphere. Tectonics 5, 227–254.

McLellan, J.G., Oliver, N.H.S., Hobbs, B.E., Rowland, J.V., 2010. Modelling fluid convection stability in continental faulted rifts with applications to the Taupo Volcanic Zone, New Zealand. J. Volcanol. Geotherm. Res. 190, 109–122.

Minissale, A., Kerrick, D.M., Magro, G., Murrell, M.T., Paladini, M., Rihs, S., Sturchio, N.C., Tassi, F., Vaselli, O., 2002. Geochemistry of Quaternary travertines in the region north of Rome (Italy): structural, hydrologic and paleoclimatic implications. Earth Planet. Sci. Lett. 203, 709–728.

Nappi, G., Renzulli, A., Santi, P., Gillot, P.Y., 1995. Geological evolution and geochronology of the Vulsini Volcano District (Central Italy). Boll. Soc. Geol. Ital. 114, 599–613.

Newman, G.A., Gasperikova, E., Hoversten, G.M., Wannamaker, P.E., 2008. Three-dimensional magnetotelluric characterization of the Coso geothermal field. Geothermics 37, 369–399.

Oliver, N.H.S., 1996. Review and classification of structural controls on fluid flow during regional metamorphism. J. Metamorph. Geol. 14, 477–492.

Oliver, N.H.S., McLellan, J.G., Hobbs, B.E., Cleverley, J.S., Ord, A., Feltrin, L., 2006. Numerical models of deformation, heat transfer, and fluid flow across basement-cover interfaces during basin-related mineralization. Econ. Geol. 101, 1–31.

Passerini, P., 1964. Il Monte Cetona (prov. di Siena). Boll. Soc. Geol. Ital. 83, 219–338.

Peccerillo, A., 2003. Plio-Quaternary magmatism in Italy. Episodes 26, 222–226.

Petit, J.P., 1987. Criteria for the sense of movement on fault surfaces in brittle rocks. J. Struct. Geol. 9, 597–608.

Piscopo, D., Gattiglio, M., Sacchi, E., Destefanis, E., 2009. Tectonically-related fluid circulation in the San Casciano dei Bagni-Sarteano area (M. Cetona ridge-Southern Tuscany): a coupled structural and geochemical investigation. Ital. J. Geosci. (Boll. Soc. Geol. Ital.) 128, 575–585. http://dx.doi.org/10.3301/IJG.2009.128.2.575.

Rosenbaum, G., Gasparon, M., Lucente, F.P., Peccerillo, A., Miller, M.S., 2008. Kinematics of slab tear faults during subduction segmentation and implications for Italian magmatism. Tectonics 27. http://dx.doi.org/10.1029/2007TC002143.

Rossetti, F., Balsamo, F., Villa, I.M., Bouybaouenne, M., Faccenna, C., Funiciello, R., 2008. Pliocene_Pleistocene HT-LP metamorphism during multiple granitic intrusions in the southern branch of the Larderello geothermal field (southern Tuscany, Italy). J. Geol. Soc. Lond. 165, 247–262.

Rossetti, F., Aldega, L., Tecce, F., Balsamo, F., Billi, A., Brilli, M., 2011. Fluid flow within the damage zone of the Boccheggiano extensional fault (Larderello–Travale geothermal field, central Italy): structures, alteration and implications for hydrothermal mineralization in extensional settings. Geol. Mag. 148, 558–579.

Rowland, J.V., Sibson, R.H., 2004. Structural controls on hydrothermal flow in a segmented rift system, Taupo Volcanic Zone, New Zealand. Geofluids 4, 259–283.

Savelli, C., 2001. Two-stage progression of volcanism (8–0 Ma) in the central Mediterranean (southern Italy). J. Geodyn. 31, 393–410.

Serri, G., 1997. Neogene–Quaternary magmatic activity and its geodynamic implications in the Central Mediterranean region. Ann. Geofis. 40, 681–703.

Sheldon, H.A., Ord, A., 2005. Evolution of porosity, permeability and fluid pressure in dilatant faults post-failure: implications for fluid flow and mineralization. Geofluids 5, 272–288.

Sibson, R.H., 2000. Fluid involvement in normal faulting. J. Geodyn. 29, 469–499.

Sibson, R.H., 2001. Seismogenic framework for hydrothermal transport and ore deposition. Rev. Econ. Geol. 14, 25–50.

Traineau, H., Sanjuan, B., Beaufort, D., Brach, M., Castaing, C., Correia, H., Genter, A., Herbrich, B., 1997. The Bouillante geothermal field (F.W.I.) revisited: new data on the fractured geothermal reservoir in light of a future stimulation experiment in a low productive well. PROCEEDINGS, Twenty-second Workshop on Geothermal Reservoir Engineering Stanford University, Stanford, California, January 27–29, SGP-TR-155.

Wedepohl, K.H., 1995. The composition of the continental crust. Geochim. Cosmochim. Acta 59, 1217–1239.

Wise, D., Funiciello, R., Parotto, M., Salvini, F., 1985. Topographic lineament swarms: clues to their origin from domain analysis of Italy. Geol. Soc. Am. Bull. 96, 952–967.

Wood, C.P., 1994. Aspects of the geology of Waimangu, Waiotapu, Waikite and Reporoa geothermal systems, Taupo Volcanic Zone, New Zealand. Geothermics 23, 401–421.